PONTIFICIA UNIVERSIDAD CATÓLICA DEL PERÚ

ESCUELA DE POSGRADO

CONTROL FOR AN ACTIVE MAGNETIC BEARING MACHINE WITH TWO HYBRID ELECTROMAGNET ACTUATORS

THESIS TO CHOOSE THE ACADEMIC DEGREE OF MAGISTER IN INGENIERÍA MECATRÓNICA

Presented by:

JOHN HUGO LOZANO JAUREGUI

Advisors : Ph. D., Ing. JULIO CESAR TAFUR SOTELO

MSc. JESUS ALAN CALDERÓN CHAVARRI

Dpl. Ing. ELISEO BENJAMÍN BARRIGA GAMARRA

MAY 2021

Lima- Perú

SUMMARY

This thesis work begins with the revision of state of the art about active magnetic bearings (AMB), the mathematical methods used to obtain geometric and physical parameters that will influence in the mechanical, electrical design and control system proposed by this prototype.

The control system will activate the magnetic bearing to center its shaft, for which it is joined a variable load in order to study the best control performance under different load over the rotor proposed by requirements. When the rotor is not controlled in its own axis even though variable load, a position error will occur that will be corrected by the program of a control system that will center the shaft (rotor).

For this design was evaluated generalized AMB models [2], [3], [4] to validate the best identification for this design, furthermore as a consequence to get the best performance for the control system as it was achieved by generalized models and it was evaluated the advantage of this AMB machine through "Two hybrid electromagnet actuators" and variable load fixed to its shaft. For this reason, it was necessary to test a simple AMB with only one electromagnet actuator [4], due to compare enhancement of hybrid characteristics for the electromagnet actuators, for which, also it was evaluated how many actuators could be necessary to join to an AMB system with the target to get the control. It means, in this work there are comparisons between a simple AMB, generalized AMB models and this design, owing to show the achievements of this design.

In order to show experimental results in state of the art, it is known that Siemens presented Simotics Active Magnetic Bearings technology for wear free operation in large – machine applications, regulated magnetic fields hold the rotor in suspension precisely without oil or contact, to make this task, sensors capture the position of the shaft 16000 times per second and a regulator adjusts the magnetic field to keep the rotor hovering precisely in the bearing center [1].

By other side the author [4] describes the experimental results in which is proposed that at low speed the bearing parameters are mainly determined by the controller characteristics.

While at high speed, the bearing parameters are not only related to the control rule but also related to the speed. This may be due to the influence of eddying effect. [4]

Furthermore, by author [3], the algorithm to get fast responses in front of disturbances, the disadvantages of these algorithms are given by not enough memory space to execute them, due to computing time is short compared with rotor displacement response time, and it is defined that it could be possible to execute the control algorithm through a real-time operating system to obtain the desired response [3].

Finally, in reference [6] it is described about filtering every noise as additive white Gaussian noise, by a predictive filter, which is obtained by analyzing Least Mean Square (LMS) and feedback/feedforward algorithm.

DEDICATION

To my parents Hugo and Mildred, who guide me on the path of knowledge and my uncle Pedro, for his teachings for life.

GRATEFULNESS

My special thanks to my advisor, Ph.D. Julio Cesar Tafur Sotelo, the Dpl. Eng. Eliseo Benjamín Barriga,Gamarra, for the unconditional support to make and build the AMB machine, as well as my co-advisor, the MSc. Jesus Alan Calderón Chavarri, who gave me all the mathematical and experimental help to bring results in this study.

TABLE OF CONTENTS

LIST OF SYMBOLS

R : Rotor reaction force [N] m

: Mass [kg]

□ : Angle of deviation of the rotor to the z-axis [°]

Ɵ : Angle of deviation of the rotor to the axis [°] g

: Force of gravity. [N]

α : Angle between the reaction force of the rotor and the rotor shaft.[°]

I : Current [A]

L : Shaft length [cm]

INTRODUCTION

Nowadays, innovation is implementing many scientific fields, including science and technology.

The objective of innovation is to find resources that reduce the inputs, components or tools used in the field of industry, one of the many elements of machines is the rotor, which rotates on bearing supports.

Continuous use, high speeds, the turning power of the rotors of machines change their operation with respect to the loads they support, this generates the problems of efficiency and wear [3].

Bearings are plenty used in different areas of engineering, such as automotive, robotics, machine CNC (computer numerical control) etc. Notwithstanding, their applications are not simple due to intricate environment like heat produced through friction increase working conditions. For this reason, in order to choose a kind of bearing, it must to be known its material properties, advantages and disadvantages, which generates a current technical problem [6].

Although there has been a high level of technical quality in the development of bearings, there are deficiencies because of wear (as friction consequence), maintenance and lubrication, which reduce its rotation speeds [3].

The solution for these problems would be by improving the traditional mechanics bearings through hybrids magnetic bearings, this function is based on the principle of passive magnetic suspension of ferromagnetic body that (is stabilized) in positions by forces of magnetic attraction after that it is needed more magnetic force and control of these forces, obtained by electromagnetic coils.

The reason is avoiding mechanical friction, the active magnetic bearing makes more efficient because it does not need maintenance which makes it very efficient in all technological fields such as turbines, vacuum pump, cryogenic technology, biotechnology, robotics, milling machines, nuclear and space installations [3].

It was designed a hybrid magnetic bearing in PUCP (student thesis developing in parallel to this work: Bjorn Henrich, Enrique Aguilar) as a consequence of previous researches [6], from which was possible to study its physical parameters, geometrical characteristics owing to design the control algorithm to achieve its desired position as requirements proposed in this thesis. The target of the magnetic bearing means to center its shaft in parallel to its imaginary axis while rotating movement, even though load added to the shaft. As a consequence, the result that was looking for avoiding wear due to friction reduction furthermore to attenuate shaft vibration, for this reason the purpose of this thesis is “Design, the control of two magnetic bearings” through a right identification system and an appropriated control algorithm for this hybrid AMB machine, and the specific objective is compare two controllers for the system, such as proportional integral derivative controller (PID) and optimal controller.

The position signals captured by position sensors when the rotor rotate around its imaginary axis produce an error while it is compared with desired (required) position, therefore the control system regulates the rotation stability on its axis, avoiding the friction. The main impact is that the motor provides maximal power through the shaft because of no friction on the movement transmission, this improves energy transmission at required RPM.

CHAPTER 1

DESCRIPTION OF ACTIVE MAGNETIC BEARING

Active Magnetic Bearings are design to reduce the friction, the constant use of lubrication in rotating machines, losses and pollution of the environment [9]. In this chapter, it will show the classification of bearings and magnetic bearings, their components and function as a prototype, in the same way machine.

1.1. Bearing

Bearing is a mechanical element shown in Figure 1.1 found in all machines where are gears, its function is to reduce the friction between an axle and the parts connected to it by means of a rolling, which serves as support and facilitates its movement.

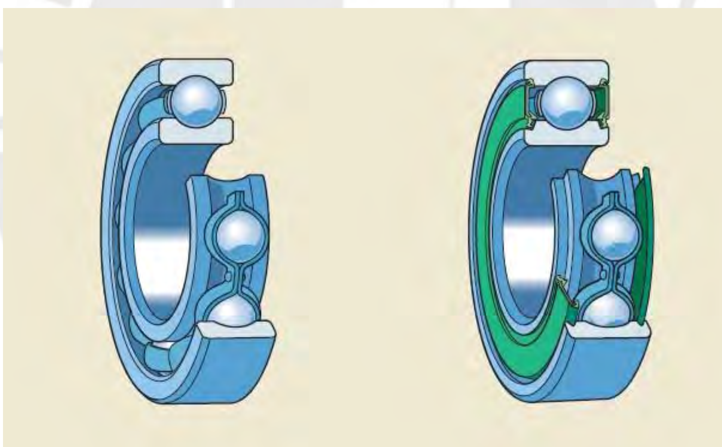

Figure 1.1: Mechanical bearing designed by SKF [1]

1.2 Mechanical support

Mechanical support shown in Figure 1.2 is considered a unit that includes at least one bearing or more, that supports an axial load rotational movement by means of the fixation of some bearings.

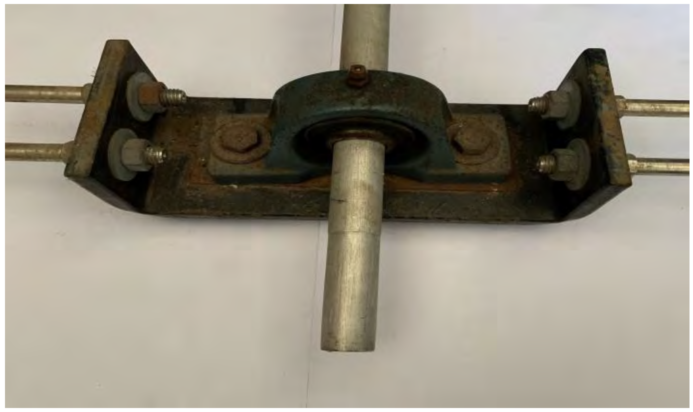

Figure 1.2: Mechanical support with mechanic bearing SKF [1].

1.3 Types of bearings

Depending on the type of contact, in the Figure 1.3, bearings can be fabricated by ball bearings (3a), cylinders (3b), sliding(3c), bearings that are constantly lubricated(3d) and the type where there is no contact which are the magnetic bearings due to magnetism. [1].

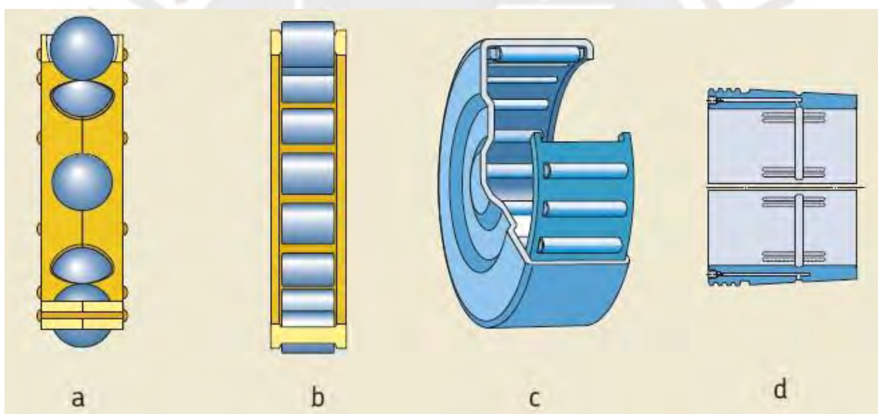

Figure 1.3: Classification of mechanic bearing SKF [1].

1.4 Magnetic permeability

Magnetic permeability is the relative increase or decrease of the magnetic field of a body compared to another body of the same or different material. Magnetic permeability is determined as the magnetic flux of a material between a magnetic field [5].

1.5 Lorentz force

The Lorentz force is generally used to produce torque in electric machines such as motors to initiate the movement of an axis.

1.6 Maxwell force

Maxwell´s force is hidden by the magnetic suspension technique that is produced by electromagnetic forces that are controlled by an electric circuit.

1.7 Flotor

Flotor is a type of term that suggests that there is a magnetic levitation. This case is found when there is an axis floating due to electromagnets, this axis is called a float.

1.8 Magnetic levitation

Magnetic levitation is a position without any mechanical contact shown in Figure 1.4, where the gravitational force is balanced only by magnetic forces. The floating axis called float remains stable by means of forces that are produced by electromagnets. [5]

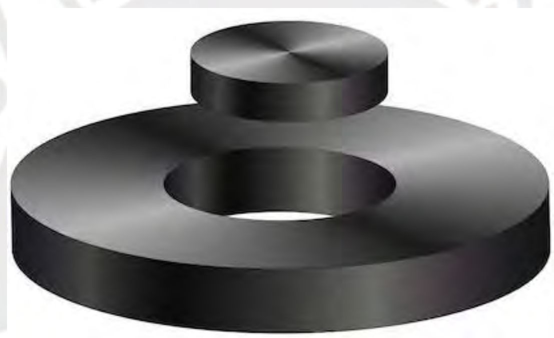

Figure 1.4: Magnetic levitation without contact.

1.9 Principles of magnetic bearing functions

In the magnetic bearings there are interacting components such as a sensor that measures the displacement of the rotor in the x, y, z, coordinates a microprocessor that functions as a controller derives a control signal from the measurement, by means of a power of an amplifier, this control signal is transformed into a control current, and the control current acts on the electromagnetic coils generating a magnetic field, which when these magnetic forces act carries a flare to a proposed theoretical axis[7]. The magnetic forces cause the rotor to remain in a levitating position. The law of control of feedback is responsible for stability and suspension. Stiffness and damping can vary widely according to the sensors, actuators and control system [7].

1.10 Position sensing

The use of different types of sensors is defined depending on the position of the medium where it will act and the measurement precision that will be required [5].

Among the sensors types are the following: optical sensors, capacitive sensors, eddy current sensors and inductive sensors.

1.11 Types of magnetic bearing

1.11.1 Magnetic bearing

Magnetic bearing supports a load using magnetic fields to perform the functions of levitation shown in figure 1.5, centering and thrust control of rotor, magnetically levitating the suspended rotor as a float. The main advantage of magnetic bearings compared to mechanical bearings is that they are non- contact. Therefore, magnetic bearings don´t require lubrication and are not subject to mechanical friction wear. For applications involving high speed rotation, significant energy is lost due to friction when using mechanical bearings, while properly designed magnetic bearings exhibit near zero losses. Applications for magnetic bearings include wheel energy storage systems for intermittent sources of renewable energy, compressors, turbines, pumps, generators and motors. Compared to conventional bearings a magnetic bearing has many advantages, such as no friction, no abrasion, no lubrication, high speed, low noise, high precision, and long life. [9]

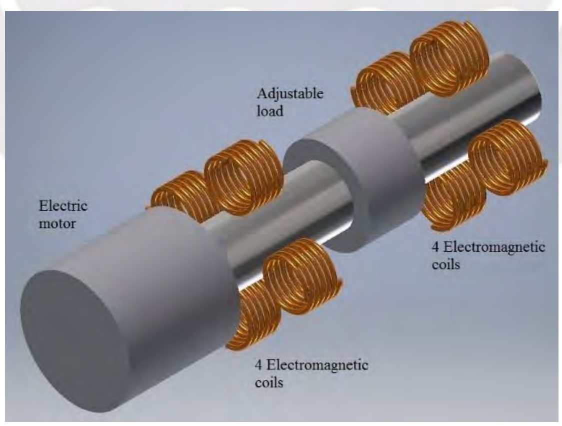

Figure 1.5: Rotor system with 2 magnetic bearings.

1.11.2 Active magnetic bearings

The active magnetic bearing consists of multiple electromagnetic coils attached to a ferromagnetic stator. In the Figure 1.6, is shown the position of the active magnetic bearing components, such as sensor gap, electromagnet, and rotor. The coils are arranged in such a way that the poles are adjacent, maximizing the magnetic flux through the rotor, a ferromagnetic is attached to the shaft to provide the flow path and attractiveness magnetic forces while minimizing the formation of eddy currents. [9]

The active magnetic bearings need a control system, that works with data obtained by position sensor, the control system regulate the electrical energy emitted by electromagnets. The disadvantage is the active magnetic system needs a constant source of electrical energy.

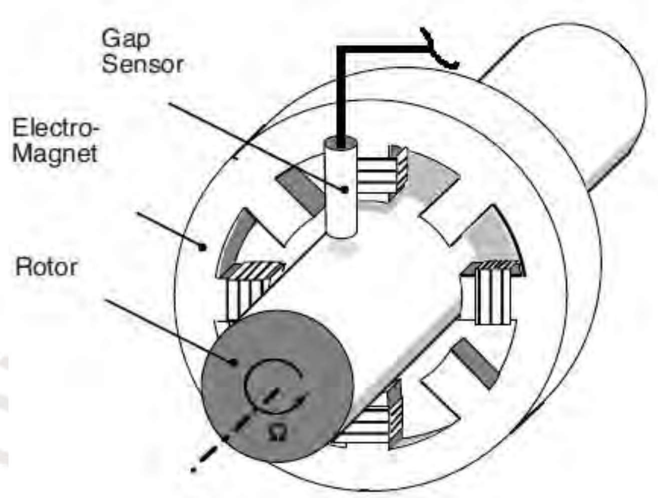

Figure 1.6: Active magnetic bearing [9].

1.11.3 Passive magnetic bearing

Passive magnetic bearings, works with magnetic field emitted by permanents magnets such as ferrite magnets and neodymium magnets. This magnetic force is not controllable. Depending on the position being implemented, stabilization in radial, axial and tilting directions is possible [9].

An advantageous feature of passive magnetic bearing is the constant suspension shown in Figure 1.7.

Figure 1.7: Passive magnetic bearing.

1.11.4 Hybrid magnetic bearing

Hybrid magnetic bearings are the operation of active magnetic bearings with passive magnetic bearings. [9]

The innovation in the industry is growing and with the passing of the years it is improving quality, performance and efficiency, in this thesis it is shown the optimization of mechanical bearings, which come to be the hybrid magnetic bearings. For the development of hybrid magnetic bearings, the following subjects are needed, which are mechanical static and dynamic, advanced mathematics to find physical and geometric parameters, control methods and software for simulation and programming. [9] For this reason in this thesis work is implement a control system for hybrid magnetic bearings using the advantages obtained from active magnetic bearing and passive magnetic bearings.

1.12 Siemens Model.

The active magnetic bearings allow a stable levitation of the rotor without contact, the levitation of the rotors is achieved by the appropriate electromagnetic forces an active magnetic bearing consists of components, sensors measure the displacement of the rotor from its reference position; a microprocessor like the controller derives a control signal from the measurement, the power amplifier transforms this control signal into a control. Current and the control current generates the magnetic forces inside the drive magnet in such a way that the rotor remain in it is suspended position [2].

Siemens company presents an active magnetic bearing system for industrial machines, such as high- speed motors, industrial turbines and compressors.

The rotors for the applications remain suspended in the center of the bearing without friction or wear. To achieve suspension, the sensors record the axis position 16,000 times per second and a controller adjust the magnetic field to keep rotor floating precisely in the center of the bearing. Exiting also on rotors weighing several tons rotating at maximum speed can be maintained in a position defined by the user. Simotics Amb technology is a highly efficient and suitable solution for large machine applications.

AMB technology from Simotics is widely used in the oil and gas industry, as well as for power generation.

But it is also a good choice for any industry that uses high performance machines and fast execution with speed electric motors. Simotics AMB technology is mainly used in compressors for the transport and storage or gas or liquefaction. [2]

Figure 1.8: Simotics AMB – Siemens Technology[2].

Reviewing the national investigations, the research thesis “Optimal control for a prototype of an active magnetic bearing system” [7], where it announces: “The implementation of the model and successful real-time control, also it is known that the implementation of its control reports high instability in low frequencies, which suggests that in high frequencies it has better results in the implemented control. In this thesis an estimator was implemented that filters the noise of the position sensor that is within all the presented control algorithms.

Furthermore, that prototype has a bearing support as it is shown in figure 1.2 [7], a DC motor, besides the electromagnets without passive magnets, as it is depicted in the figure 1.3 [7].

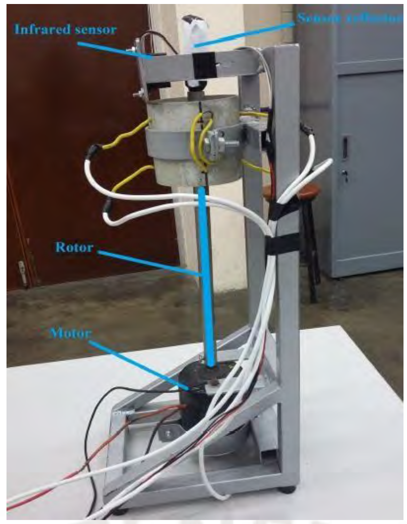

.
Figure 1.9: Parts of active magnetic bearings [7].

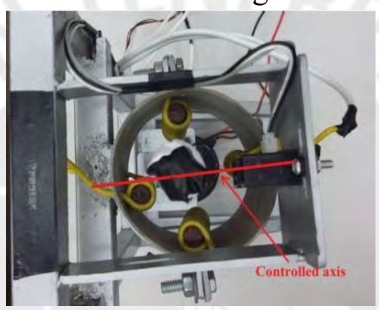

Figure 1.10: Prototype of active magnetic bearing controlling a rotor [6].

Likewise, in the research thesis: "Physical parameters identification for a prototype of active magnetic bearing system" [7], The author considers: "a simple structure with an active magnetic support in a vertical position and without gravity forces, this model allows to identify mechanical and electrical parameters to obtain an idea and identify industrial equipment. Neural networks are used to identify the parameters including configuration data and error minimization in a time if 5 seconds, then the time to identify and update the parameters is around 1.6 seconds that it is possible to include this identification within the control system.

The error of identifying parameters with neural network and transfer functions is around 3%, it is good estimate of the response. [7]

1.13 Magnetic Bearing model to develop

Futures projects include an industrial prototype with precision sensors and better control for a better accuracy in the results, considering into account the operation of an engine that only transmits torque forces and the radial impulse to design and assemble a prototype of active magnetic bearings including the central mass between them. All the aforementioned information will be considered for the study that will be developed regarding the design of two magnetic bearings to center an axis to an imaginary axis. [6]

1.14 Development of Magnetic Bearings

The active magnetic bearings for this thesis work use 4 position sensors, 8 electromagnetic coils, a variable load an engine that will transmit the movement to the rotor that will work between the magnetic bearings.

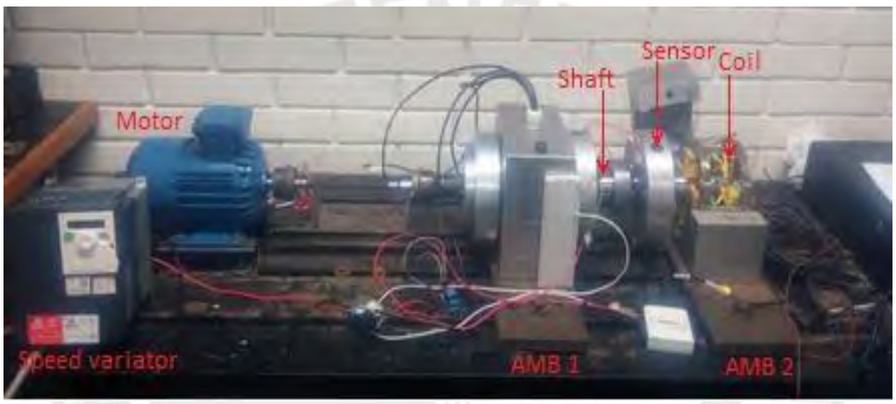

Figure 1.11: Rotor system with 2 hybrid magnetic bearings

CHAPTER 2

MATHEMATICAL MODELING FOR THE HYBRID MAGNETIC BEARING SYSTEM.

In this chapter is explained the theoretical and experimental dynamic of the hybrid active magnetic bearing system studied.

To understand the dynamic of the hybrid active magnetic bearing, it is proposed the diagram block to show in Figure 2.1, when it is used mechanical and electrical differential equations to obtain a process dynamics solution for acquire a range of physics and geometric parameters for the transfer function of the system obtaining 8 range of values "g".

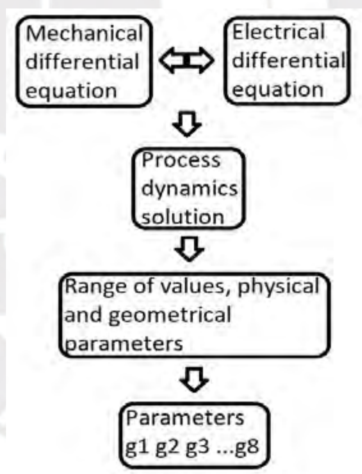

Figure 2.1: Diagram block function to obtain geometrical y physical parameters

2.1 AMB geometrical and physical parameters analysis.

In Figure 2.2 is depicted the scheme connection between the shaft, motor and electromagnets, that are main components of the hybrid magnetic bearing of this thesis.

Otherwise, its geometrical parameters are "L" which is the length of the shaft (1m), "D" is its diameter (0.3m). This scheme helps to get a general understanding to elaborate the setup in order to describe it by physical laws, besides, it is connected the DC motor, that has a power of 1Hp, with the shaft through a coupling which absorbs reaction between motor and shaft.

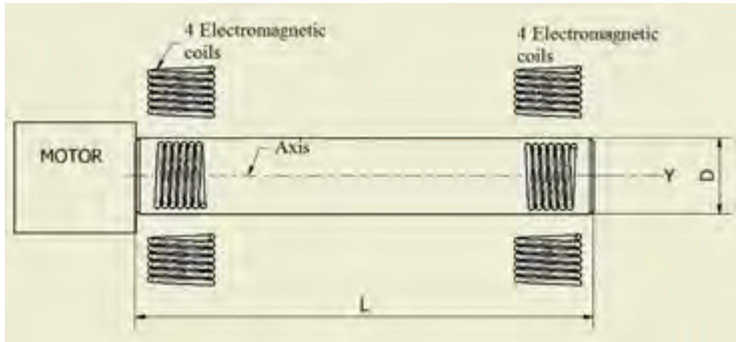

Figure 2.2: Mass with levitating rotor with magnetics bearings.

In order to propose the mathematical model of the system, it was necessary to know the physical and geometrical parameters, under requirements, for a non-flexible case, it defined 4 electromagnetic forces with resultant forces FM1, FM2, FM3, FM4, for each electromagnet shown in Figure 2.3.

Furthermore, it is necessary to describe that as consequence of not balanced system (when it is not achieved the control yet) and gravity force over rotor, the reaction get components in axis "X, Y and Z"; in otherwise, every electromagnetic force as components in every axis too as shown in Figure 2.3.

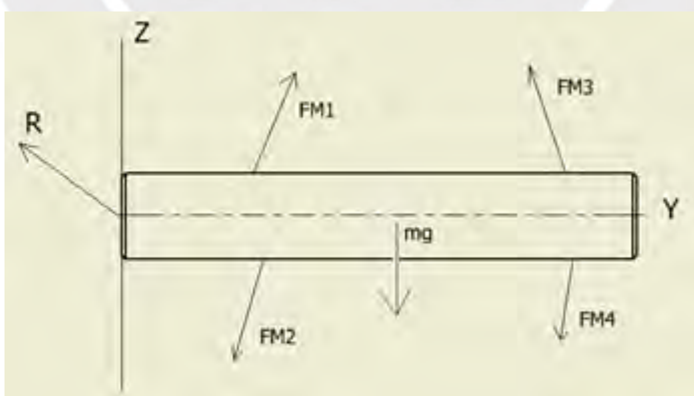

Figure 2.3: Free body diagram that apply on the rotor.

Therefore, the mathematical model for the magnetic bearing, was obtained through the proposed system, when the rotor turns itself around axis "y", and produce an angular translation ϴ.

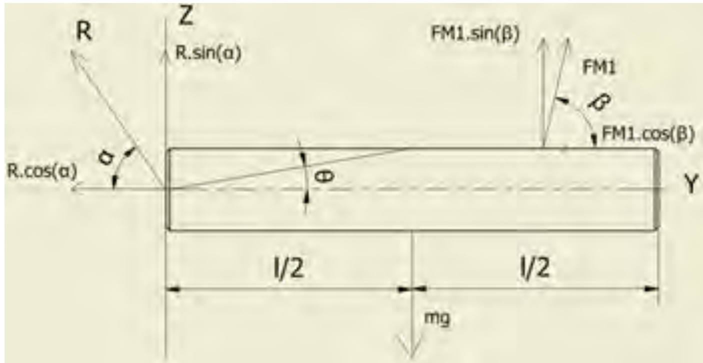

Figure 2.4: Dynamical analysis [3].

Therefore, with the static model shown in Figure2.4, for it the following equations describes the mechanics of this system. Otherwise, its physical parameters are described by physical laws.

The initial conditions in the equation (1) describes where R is a resultant force between rotor and motor, and FM is a magnetic force for one electromagnet by equilibrium rotational when the electromagnetic system is activating but the motor is off and gravity force mg, is given by initial conditions.

$$Rsin\alpha + FM1sinB - mg = 0 \ldots (1)$$

Solving equation (1) with the static condition, the sum of forces is zero, it is obtained by equation 2, 2*, decomposing the resulting force FM1, it is obtained equation 2 in axis X, and equation 2* in the axis y.

For x axis:

$$Rcos\alpha = FM1cosB \ldots (2)$$

For y axis:

$$Lmg = FM1sinB2L \ldots (2^{*})$$

Classical mechanics of balance, where the summation of forces for not translation r and for not rotation θ, because the magnet force was activated, but the rotor no yet rotate, therefore it can obtain the acceleration in (3) and (4).

While $$\begin{cases} \sum F \rightarrow \frac{\overline{d_r^2}}{d_t^2} \\ \sum F \rightarrow \frac{\overline{d_\theta^2}}{d_t^2} \end{cases} \ldots (3)$$

$$\frac{md_z^2}{dt^2} = R\sin\alpha + FM1\sin B - mg \ldots (4)$$

Where the components of equation (4), Shown the dynamic equation there are an acceleration in direction of axis z, because the equilibrium is start to be broken, the acceleration is equal magnetic force FM, R is a reaction the contact with motor to get a transmition and mg is a gravity force.

Solving the equation (1) in (4) it is obtained equation 5, were:

$$\frac{md_z^2}{dt^2} = mg - FM_{1_{(0)}} \sin B + FM_1 sinB - mg \quad \ldots (5)$$

Where magnetic force $FM_{1(0)}$ is the initial condition for the system in equation (6) were K_Z is the distance variation in millimeters, and Ki is the variation of current in amperes.

$$\frac{md_z^2}{dt^2} = (K_Z Z + K_i i) \sin B - (K_z Z_0 + K_i i_0) \sin B \quad \ldots (6)$$

The general equation for one electromagnet, the dynamic equation of z axis is:

$$\frac{md_z^2}{dt^2} = K_Z \sin B(Z - Z_0) + K_i sinB(i_i - i_0) \ldots (7)$$

The magnetic force given by the figure 2.3 is:

$$F_{Mr} = K_r r + K_i I \ldots (8)$$ It

is represented by variation of the distance and current:

$$\int_{z_0}^{z} d\, z = z - z_o \ldots (9)$$

$$\int_{i_0}^{i} d\, i = i - i_0 \ldots (10)$$

Translation equation reference are shown in the equation (11)

$$\frac{md_z^2}{dt^2} = K_Z \sin B(z) + K_i sinB(i) \ldots (11)$$

Solved the equation (11) it is obtained:

$$\frac{Id_0^2}{dt^2} = -Lmg + 2LFM1sinB \ \ldots (12)$$

$$\frac{I_Z d_\theta^2}{dt^2} = -L\big(2sinB(K_Z Z_0 + K_i i_0)\big) + 2LsinB(K_Z Z + K_0 i) \ \ldots (13)$$

Equation of rotation for the system is:

$$\frac{I_Z d_\theta^2}{dt^2} = 2LsinBK_z(Z - Z_0) + 2LsinBK_i(i - i_0) \ \ldots (14)$$

If:

$$\theta = \theta - \theta_0$$

$$\frac{I_Z d_\theta^2}{dt^2} = 2LsinBK_z(Z) + 2LsinBK_i(i) \quad \ldots (14^*)$$

$$l = L\theta \quad \text{for all } \theta \to 0 \ldots (15)$$

$$l \rightarrow Z$$

$$\frac{Iz d_{\theta}^{2}}{dt^{2}} = sinBK_z\theta + 2LsinBK_i i\ldots (16)$$

Using (11) and (16) the mechanical equation for only one electromagnet, is given by (17). [3]

$$\begin{pmatrix} m & 0 \\ 0 & Iz \end{pmatrix}\begin{pmatrix} \frac{d^2z}{dt^2} \\ \frac{d^2\theta}{d\theta^2} \end{pmatrix} - \begin{pmatrix} K_z sinB & 0 \\ 0 & K_z sinB \end{pmatrix}\begin{pmatrix} Z \\ \theta \end{pmatrix} = \begin{pmatrix} K_i sinB \\ 2LsinBK_i \end{pmatrix} \ldots (17)$$

Furthermore, using laws of Kirchhoff is obtained the equation (18) that related an electrical current with a voltage signal, the electrical current, (i) for the hybrid system be determined:

$$v = RI + L\frac{d_I}{dt} \ldots (18)$$

It means (17), (18) Mathematical model AMB

For the matrix 2 Electromagnets are shown in the matrix equation (19):

$$\begin{pmatrix} m & 0 & 0 & 0 \\ 0 & I_z & 0 & 0 \\ 0 & 0 & m & 0 \\ 0 & 0 & 0 & I_x \end{pmatrix}\begin{pmatrix} \frac{d^2z}{dt^2} \\ \frac{d^2\theta_z}{dt^z} \\ \frac{d^2X}{dt^2} \\ \frac{d^2\theta_x}{dt^2} \end{pmatrix} -$$

$$\begin{pmatrix} K_z sinB & 0 & 0 & 0 \\ 0 & K_z sinB & 0 & 0 \\ 0 & 0 & K_x sinB & 0 \\ 0 & 0 & 0 & K_x sinB \end{pmatrix}\begin{pmatrix} z \\ \theta_z \\ x \\ \theta_x \end{pmatrix} =$$

$$\begin{pmatrix} K_i sinB_z & 0 & 0 & 0 \\ 0 & 2LK_i sinB_Z & 0 & 0 \\ 0 & 0 & K_i sinB_X & 0 \\ 0 & 0 & 0 & 2LK_i sinB_X \end{pmatrix}\begin{pmatrix} i_z \\ i_z \\ i_X \\ i_X \end{pmatrix} \ldots (19)$$

The same matrix for equation (19) is the equation (20)

$$\begin{pmatrix} L_z & 0 \\ 0 & L_x \end{pmatrix}\begin{pmatrix} dI_z \\ dI_x \end{pmatrix} + \begin{pmatrix} R_z & 0 \\ 0 & R_x \end{pmatrix}\begin{pmatrix} I_z \\ I_x \end{pmatrix} = \begin{pmatrix} V_1 \\ V_2 \end{pmatrix} \ldots (20)$$

In addition to this, the nature of the magnetic force from which it is derived has been studied. The following equation (21) is obtained, the magnetic force is a function of the position and electrical current parameters give in (21)

$$Fm(x, i) = -k_s x + k_i i \ldots (21)$$

The detail of obtaining the system of equations is shown in the annexes (equation 17), from where is obtain (22):

$$\begin{pmatrix} m & 0 \\ 0 & Iz \end{pmatrix}\begin{pmatrix} \frac{d^2z}{dt^2} \\ \frac{d^2\theta}{d\theta^2} \end{pmatrix}-\begin{pmatrix} K_z sinB & 0 \\ 0 & K_z sinB \end{pmatrix}\begin{pmatrix} Z \\ \theta \end{pmatrix} = \begin{pmatrix} K_i sinB \\ 2LsinBK_i \end{pmatrix}(i) \dots (22)$$

However, in this case the system can only be described by any of the following both since it is a system of one degree of freedom.

Likewise, in the electric circuit, Ohm's Law can be proposed, taking into account the next, when voltage "v" is the resistance per electrical current "I" added, "R" is a resistance:

$$v = RI + L\frac{d_I}{dt} \dots (23)$$

Therefore, taken from the equation (12), the particular case for translation, which explains the simple system dynamics.

$$m\ddot{z} - k_z \cos(\beta)z = k_i \cos(\beta)v/R1(1 - e^{\frac{R1}{L1}(t-t0)}) \dots (24)$$

Therefore, in order to estimate the constants, it is necessary design parameters, using system identification techniques.

With this, this model will be used to define the physical model. The calculations will be analyzed in detail when selecting the preliminary project to be used later on.

2.2 Analysis of electrical equation

Analysis of 8 hybrid electromagnetic actuators positions around the rotor in the axis x,y,z; which is divided into 2 parts.

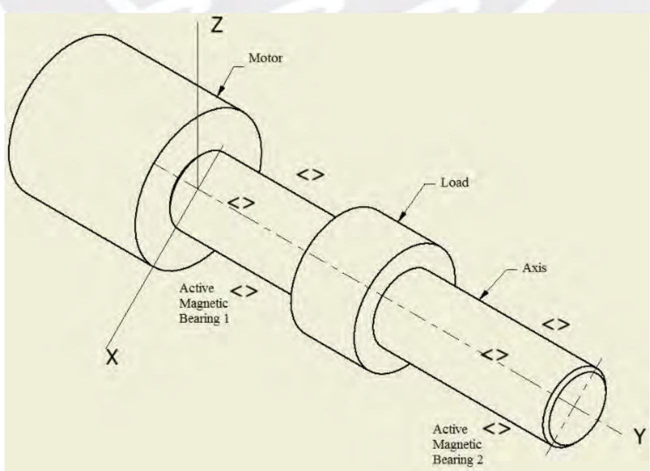

Figure 2.5: Magnetic bearing position.

For electric equation (25):

$$I_i = \frac{V_i}{R_i}\left(1 - e^{-\frac{R_i}{L_i}(t-t_0)}\right) \ldots (25)$$

It´s know the model given by:

$$m\frac{d^2x(t)}{dt^2} + \gamma\frac{\mathrm{d}x(t)}{dt^2} + kx_t = 0 \ \ldots (26)$$

System identification for the system shown in the Figure 2.5 is explained mathematically in equation (27), where define that response time(t) near 70% (it is looking for in order to avoid overshoots and to get short response time), and L is delay for excitation signal, because the hybrid magnetic bearing system has inertia, kp is the proportional constant between step response and electrical excitation. Is the proportional relation of output variable in function of the input electrical excitation showed in Figure 2.6.

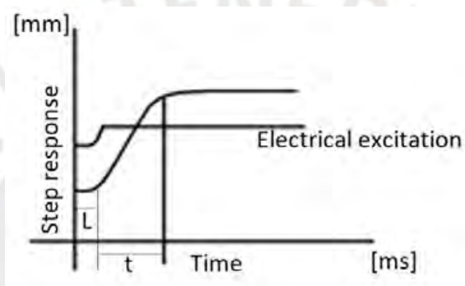

Figure 2.6 Step response and establishment point of AMB.

$$\frac{y_{(s)}}{U_{(s)}} = \frac{\mathrm{kp}}{Is+1}e^{-Ls} \Leftrightarrow L < I \ \ldots (27)$$

$$Iy_{(s)} + y_{(s)} = \mathrm{kp}U_{(s)} \ \ldots (28)$$

Where the differential equation (29) in the time domain obtained by figure 2.5:

$$\frac{Idy(t)}{dt} + y_{(t)} = \mathrm{kp}U_{(t)} \ \ldots (29)$$

For the AMB system the diferential equation in the time domain is obtained by experience:

$$\frac{ady(t)}{dt} + by_{(t)} = cU_{(t)} \ \ldots (30)$$

Modulated Functions in equation (31)

$$a_1d^n\frac{p(t)}{dt^n} + a_2d^{n-1}\frac{p(t)}{dt^{n-1}} + a_3d^{n-2}\frac{p(t)}{dt^{n-3}} + \cdots am = F(t) \ \ldots (31)$$

Responses in time by excitation (frequencies or spectrum, depends on the type of calibration) Analysis for rotation tendency with degree of freedom, in equation (32) shown the electrical current I, mass m. [3]

$$\begin{pmatrix} m & 0 \\ 0 & I \end{pmatrix}\begin{pmatrix} \frac{d^z(t)}{dt^2} \\ \frac{d^z\theta_2(t)}{dt^2} \end{pmatrix} - \begin{pmatrix} k_z sinB & 0 \\ 0 & k_z sinB \end{pmatrix}\begin{pmatrix} z \\ \theta_z \end{pmatrix} = \begin{pmatrix} k_i sinB & 0 \\ 0 & 2l sinBki \end{pmatrix}\begin{pmatrix} i_z \\ i_0 \end{pmatrix} \ldots (32)$$

For the active magnetic system, the resultant forces are emitted by each hybrid electromagnetic coil, which is shown in Figure 2.7, where FMz is the electromagnetic force resulting from an electromagnetic coil with an angle β and for another electromagnetic coil FMz2 is electromagnetic force resulting with an angle β2 , and the resultant force between rotor and motor is R, with an angle θ

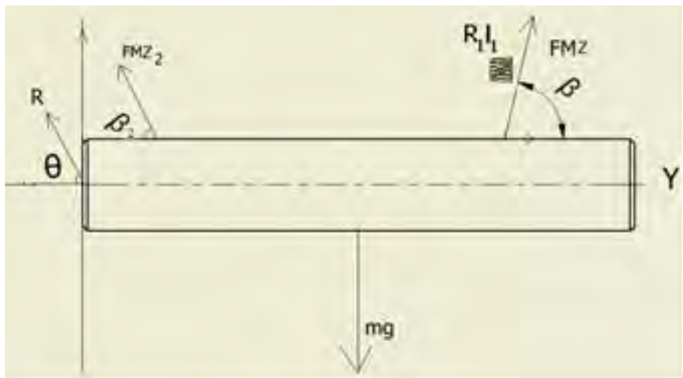

Figure 2.7: Sample of the shaft with a force that is produced by 2 active magnetic bearings.

$$md^2\frac{z(t)}{dt^2} - k_z sinBZ_t = k_i \sin Bi_b \ldots (33)$$

$$md^2\frac{z(t)}{dt^2} - k_z sinBZ_t = k_i \sin B[\frac{v_0}{R}\left(1 - e^{\frac{-R_1}{L_1}(t-t_0)}\right)] \ldots (34)$$

Therefore, to solve this differential equation to archive geometrical parameters for one electromagnet effect.

$$Z(t) = z_h^{(t)} + z_P^{(t)} \ldots (35)$$

The general equation for the system is given by equation 36:

$$md^2\frac{z(t)}{dt^2} - k_z sinBZ_{(t)} = k_i sinBi_{(t)} \ldots (36)$$

Where:

m- is a mass

Bi- is the angle between the magnetic force and the axis.

$md^2\frac{z(t)}{dt^2}$: Is the mass multiplying the derivative of the position

2.3 Analysis of electrical components:

Initial conditions:

$$i_0 \rightarrow mg \ldots (37)$$

"ϴ" it is flexible

$$\Theta \rightarrow 45°$$

$$[k_i]\sim 1$$

In the Figure 2.8 shown the linearization between the magnetic force and the current, where the initial load has the initial uses initial value of current i_0, when the magnetic force increase, the electrical energy increase.

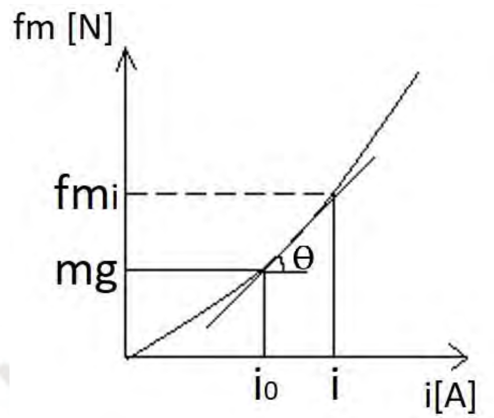

Figure 2.8: Linearization between the magnetic force and the current.

Where for the system it considers mass as 1 kg: mg→

1kg i0=10A

$$i = \in [10 \ldots 30]A$$

For Kz

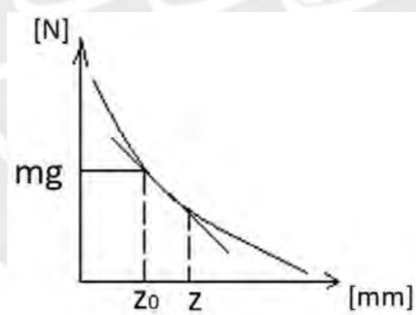

Figure 2.9: Linearization between the magnetic force (T) and distance (mm).

Trend lineal:

$$F_{Mz} \rightarrow k_Z(Z - Z_0) \ldots (38)$$

Magnetic force:

$$F_M = f_{mi} + f_{mz} \ldots (39)$$

$$F_M = k_i(i - i_0) + k_z(z - z_0) \ldots (40)$$

$$0.5\, mg = (i - 10) + (z - z_0) \ldots (41)$$

$z = 0.001m$… requirement

$z_0 = 0.0003m$.. proposal

$$5 = i - 10 + 0{,}007$$

$$i \sim 14.993$$

The magnetic force to raise 1kg, depends on the current, which according to calculations made it is defined that, the diameter of the isolated wire conductor should be ≤ 1mm and the amperage is between 10A to 20A.

Use differential equation for a one point:

$$z_{(t)} = \left(Ae^{\sqrt{k_z B_t}} + Be^{-\sqrt{k_z B_t}}\right) + \left(D + Ee^{-\mathrm{gt}}\right) \ldots (43)$$

Z regarding time:

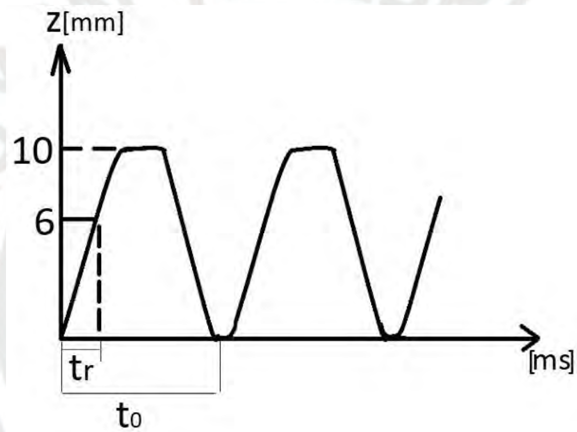

Figure 2.10: Regarding time in Z(mm) and operation time (ms).

$$tr_{computer} < tp \leq tm < tr_{sensor} < to < 200ms$$

Where shown this in the Figure (2.9) the computer time ($tr_{computer}$) response is minor than processing time (tp), the processing time, is minor equal than sampling time (tm) in the same way, sampling time must be minor tan response time sensor (tr_{sensor}) considering that response time sensor is minor than operation time (to) and the operation time is minor than 200 ms.

2.4 Analysis of magnetic permeability.

Reference to the calculations made, the following is defined:

Magnetic permeability, magnetic field strength(H) [3]:

$$i \sim 14.993$$

$$H = \frac{0.4\pi n I}{L} \ldots (44)$$

Where: n°: number of turns of a solenoid

L: length

I: current

$$n = \frac{0.4\pi I}{L\,H} \ldots (44^{*})$$

$$n = \frac{0.4\,\pi 14.993}{30H}$$

$$n = 6 \text{ turns}$$

The magnetic field increase outside the solenoid is due to the sum of the field generated by the solenoid and the magnetic field end to the magnetized bar, this new field is called magnetic induction or induction flux density.

$$B = \mu_0 H + \mu_0 M \ldots (45)$$

M: component of the field due to the bar, intensity of magnetization. μ_0 : Free space permeability

$$\mu_0 = 4\pi 10^{-7} T \cdot \frac{m}{A} \ldots (45^*)$$

$T \cdot \frac{m}{A}$: Tesla meter by ampere.

Types of conductive wires.

Conductors electrolytic cooper 99.99% minimum purity, annealed hard, the solid is chosen since the wiring generates a lot of heat.

In conclusion with the respective calculations a cooper wire that can withstand 30 amps will be implemented.

Calculation to determine the diameter of the wire:

Safety factor: 25%

$$d = 30 + 25\%\,(30) = 37.5A$$

It is defined that the type of wire is 6 awg with a diameter of 4.11 mm with an electrical resistance of 1.293934 ohms/km

2.5 SENSOR

To choose the position sensor to be used in the prototype of a magnetic bearing, the following types of sensors are proposed: position sensor, induction sensor and nanosensors, each sensor will emit parameters with a margin of noise and error, and by obtaining this data the comparison will be made to define which sensor is the optimum for the prototype presented.

2.5.1 Position sensor

Proximity sensors are switches because they determine the presence- absence of an object. This means that they produce a digital output or on/off instead of a continuous measurement of the position. In this thesis it will focus of the position sensors and not on the switches. In other words, the sensors emit an electrical signal proportional to the position along a measurement path. [14]

2.5.2 Induction sensor

When comparing the position sensors, the inductive sensors can move the electronics away from the detection area.

That allows the sensor to be placed in hostile environments and its electronics in another position less adverse. [14]

2.5.3 Nanosensors.

The use of nanosensors for the proposed prototype is the efficiency of the response of the data obtained, with the nanosensor will be obtained position variation measurements with high precision that will optimize the responses of each parameter to perform the optimal control of the prototype [3]

CHAPTER 3

Control position for the AMB

In order to achieve the control position for the hybrid AMB machine of this thesis, it is described its control analysis as dependence of mechanical and electrical subsystem

3.1 Control analysis

To develop the control, it is known a block diagram for a system AMB [3] which is shown in Figure 2.1, where I(s) is an electrical excitation signal, O(s) is the response signal, C(s) is the controller, MT(s) is the mechanical plant´s transfer function for the system, and S(s) is the transfer function for the sensor. It is necessary to remember the sampling time was less than response time of the system as requirement of this work, therefore Laplace analysis helped to algebra operation.

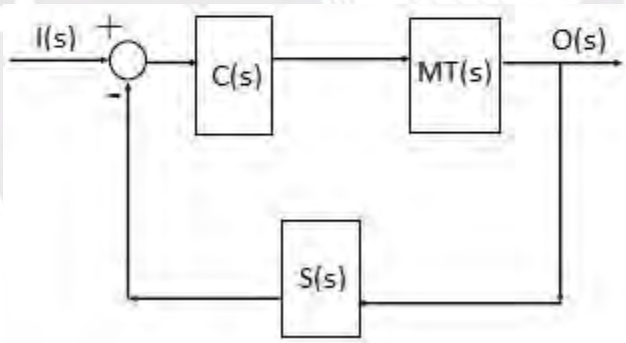

Figure 2.1 Block diagram of the identification system.

By algebra is obtained from the block diagram, the equation 46, for which "O" means the output of the system:

$$[I(s) - S(s)O(s)]\,C(s)MT(s) = O(s) \; ... (46)$$

From which it is achieved equation 47:

$$\frac{O(s)}{I(s)} = \frac{C(s)MT(s)}{1+C(s)MT(s)S(s)} \; ... (47)$$

In last equation, for a case PID controller, it is considered sensors, actuators and controller system, nevertheless for this work it is considered an enough fast response in order to assign a gain behavior, so the transfer function it is considered as S(s)=K_s therefore in the characteristic equation for a classic PID model is reduced at following equation, in that "m" represented shaft's mass. Electrical current coefficient K_i and displacement coefficient K_y. From [3] was analyzed the general case, therefore from that reference it was reduced poles numbers for this specific case 8 electromagnets the transfer function as K_i for 8 actuators separately, is the integral constant of the PID controller.

$$(K_P + \frac{K_i}{S} + K_d\, S)(\frac{K_i}{m\, S^2 + K_y}) + 1 = 0 \; ... \; (48)$$

as reduction equation (48):

$$(m\, S^2 + K_y)(\, K_d\, S^2 + K_p S + K_i)\, K_I K_S + mS^2 + K_y = 0 ... \; (49)$$

Working for a PI Controller, that means: [3], were K_p is a proportional constant,K_i is the constant of current, and K_s is a constant of sensor.

$$S^3 + \frac{(1 + K_i K_y K_y)}{K_p K_i K_s} S^2 + \frac{(K_y K_p K_i K_s)}{m K_p K_i K_s} S + \frac{K_y (K_I K_i K_s + 1)}{m K_p K_i K_s} = 0 \; ... \; (50)$$

While it is compared with third order polynomial model, it is necessary to recognize "ω_0" as the natural frequency assumed (expected for the system, "ϵ" as the capacity to overcome inertia (as damping effect) and "α" the coefficient which joins equations (49) and (50), to get comparison with main polynomial model showed in equation (51). As it was analyzed for the author for a generalized case so in this context the redactions are for 8 degrees of Freedom in given equation in which every component has a matrix 8x8. [3],

$$S^3 + \omega_0 (2\epsilon + \alpha) S^2 + \omega_0^2 (1 + 2\epsilon\alpha) S + \alpha\, \omega_0^3 = 0 \; ... \; (51)$$

Otherwise, $K_p K_I$ and α can be obtained as functions of "ω_0" and "ϵ"

$$\frac{(1 + K_i K_y K_y)}{K_p K_i K_s} = \omega_0 (2\epsilon + \alpha\,) \; ... \; (52)$$

$$\frac{(K_y K_p K_i K_s)}{m K_p K_i K_s} = \omega_0^{\,2} (1 + 2\epsilon\alpha) ... \; (53)$$

$$\frac{K_y (K_I K_i K_s + 1)}{m K_p K_i K_s} = \alpha\, \omega_0^{\,3} ... \; (54)$$

From equations (52), (53), (54) it is obtained: [3],

$$\alpha = \frac{1}{2\epsilon} - \frac{K_y}{2m\epsilon} ... \; (55)$$

it means

$$K_i = \frac{(m\omega_0 - K_y)\alpha - 2K_y\epsilon}{K_y K_I (K_s - m\omega_0)\alpha - 2K_I K_y K_s \epsilon} \ldots (56)$$

For this reason, was possible to find K_i: [3],

$$K_i = \frac{(m\omega_0 - K_y)\frac{1-\frac{K_y}{m\omega_0{}^2}}{2\epsilon} - 2K_y\epsilon}{K_y K_I (K_s - m\omega_0)\frac{1-\frac{K_y}{m\omega_0{}^2}}{2\epsilon} + 2K_I K_y K_s \epsilon} \ldots (57)$$

Therefore [3],

$$K_p = \frac{K_I K_y K_s + \frac{K_I}{K_i}}{m K_s \omega_0{}^3 \alpha} \ldots (58)$$

And finally, was possible to get the controller PI defined by its parameter proportional and integrative. This controller helps to find the right identification while system is stable.

$$K_p = K_Y K_I K_s + K_I[1 + \frac{4\epsilon^2 (K_S K_I - 1)}{K_I (K_s - m\omega_0)\left(1 - \frac{K_I}{m\omega_0{}^2}\right) - 4K_S \epsilon^2}] \ldots (59)$$

3.2 Model Predictive Control Analysis

Results obtained in this thesis work help to get a control under requirements looked for, nevertheless, not fast response as it could be obtained by a predictive model, either way such as by an Optimal Predictive Control described in following lines. For this reason, it was studied, simulated and experimented by optimal analysis for the main control in this thesis.

The heating propagation because of friction in bearings is a problematic that can be improved while the AMB is controlled by an optimal PID controller, which coefficients are calculated by analysis of strategic solutions of the optimal models that represents the main system in this work (electromechanical system) [3]. That means, in this research was necessary to work with strategies of Model Predictive Control (MPC) joining both subsystems (mechanical and electrical) for the main algorithm, the strategy was an internal identification system while adaptive control coefficients/weights looked for the right control. Therefore, it is generalized for a nonlinear function “f” and internal variables “x(t)” due to excitation “u(t)” as function to time “t” As it was analyzed for the author for a generalized case so in this context the redactions are for 8 degrees of Freedom in given equation in which every component has a matrix 8x8.

$$\frac{dx(t)}{dt} = f(x(t)u(t), \Theta) \ldots (60)$$

By other side the general response “y(t)” correlated with “x(t)” and “u(t)” through a nonlinear function “h”

$$y(t) = h(x(t), u(t), \Theta) \ldots (61)$$

Also, while trajectory road “Rs” as input excitation “r”

$$R_s^T = (11111111)r(k_i) \ldots (62)$$

So, analyzing costing function “J”, according to achieve the optimal desired position. [3],

$$J = (R_S - Y)^T(R_S - Y) + \Delta U^T R \Delta U \ldots (63)$$

In which this expected position is

$$Y = FX(k_i) + \phi\Delta U \ldots (64)$$

Otherwise, [3],

$$_T{}^T\phi^T(R_S - FX(k_i)) + \Delta U^T(\phi^T\phi + R)\Delta U \ldots (65)$$

$$J = (R_S - FX(k_i))\ (R_i - FX(k_i)) - 2\Delta U$$

In that, “F” and “ϕ” are matrices that contain all physical parameters of the system (as joining matrices above regard identified result). [3],

$$\frac{\partial J}{\partial \Delta U} = -2\phi^T((R_S - FX(k_i)) + 2(\phi^T\phi + R)\Delta U \ldots (66)$$

So

$$\frac{\partial J}{\partial \Delta U} = 0 \ldots (67)$$

From which, the optimal excitation signal in order to find the optimal response is given by [3],

$$\Delta U = (\phi^T\phi + R)^{-1}\phi^T(R_S - FX(k_i)) \ldots (68)$$

The total systems (mechanical and electrical subsystem) were controlled through following scheme of general cascade controller as shown in Figure 2.2 by [3], in which “G_1 and G_2” are the controllers, furthermore, “G_3 and G_4” are the subsystems of all the AMB model.

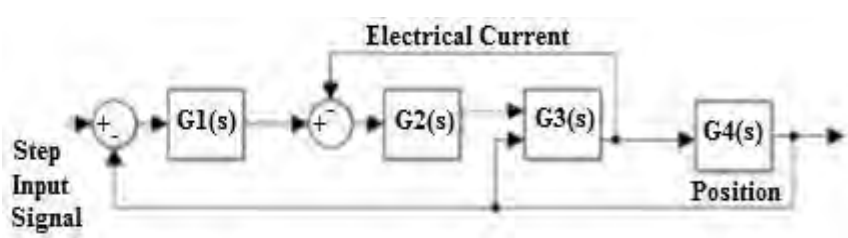

Figure 2.2 Control cascade model for the total system.

CHAPTER 4

SIMULATION RESULTS

4.1 Control position results

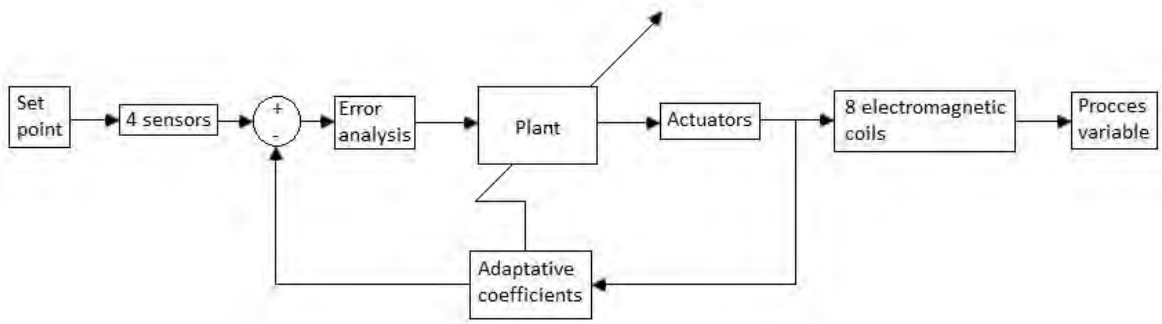

Figure 4.1 System control scheme for simulation of hybrids magnetic bearings.

It was achieved the control by experimental analysis as consequence from simulations achieved, as it is depicted in Figure 4.2, for which the curve in color black shows shaft rotation while there is not magnetic force influence, it because of any hybrid electromagnet actuator was activated. Therefore, it is possible to see impulses such as overshoots which give as result the necessity to get a position control in order to get movement stable and balanced transmission; furthermore, it is shown by green curve the result of the main control designed while it is activated only one of the hybrid electromagnet actuators, besides by red line it is shown better performance (reduced overshoots) owing to the position sensor measure rotor movement while there is activated both hybrid electromagnet actuators. That means, the simulation expected best performance control when the main algorithm is executed when both actuators are activated, it likes to be owing two load between both actuators.

By other side, in order to test simulation results, there are shown figure 3.3 and figure 3.4 to describe experiments results achieved.

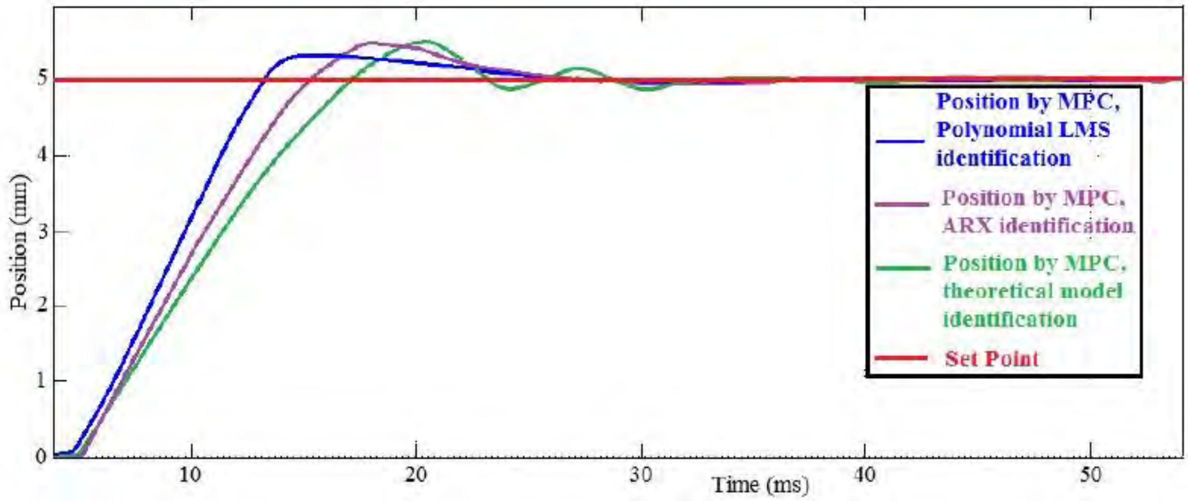

Figure 4.2 Model Predictive Control Simulation result (as dependence of identification methodologies) for the AMB prototype. [3]

In magnetic bearings system, the results of a system comparison are shown in Figure 4.3, without control, with control of an actuator and with control of two actuators, where the position sensor senses the y axis and is obtained the signal of black color, which indicates that there is no control in the system, and its oscillation is 1.38 mm to 1.42 mm and 1.32 mm to 1.50 mm maximum. When activating the control system with an actuator, the green signal is obtained, decreasing the oscillation between 1.39 mm to 1.41 mm, which is a range attenuated to the imaginary axis. In the same way a second actuator is activated, in vertical position to the first, giving a red signal, which greatly influences the attenuation obtaining an oscillation of 1.305mm to 1.405 mm, values that approximate the imaginary linear axis.

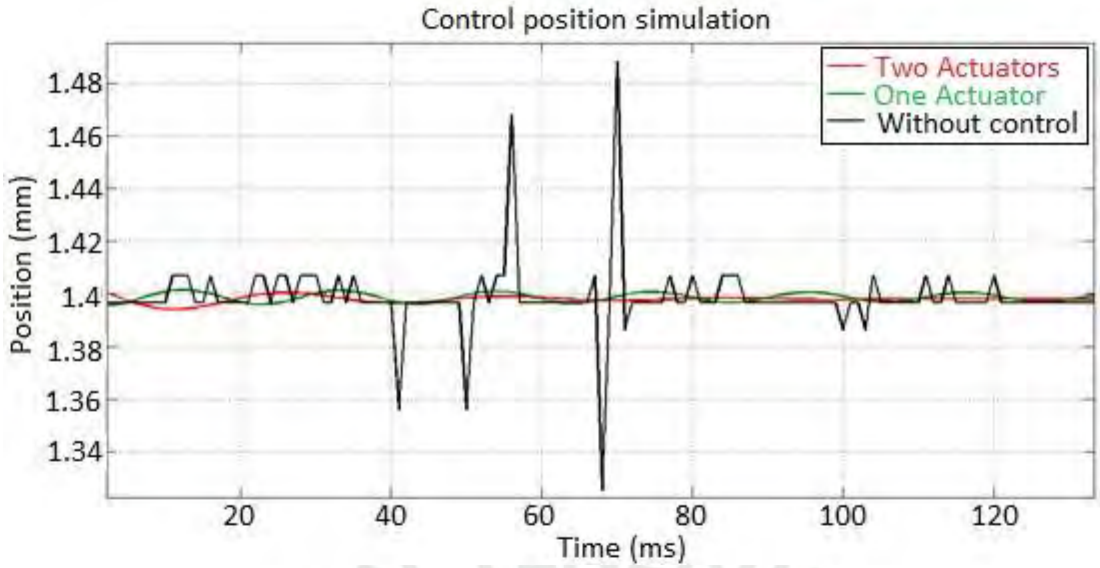

Figure 4.3 Comparison between the signals emitted, without control, with control of an actuator and with control of two actuators.

CHAPTER 5
Experimental results

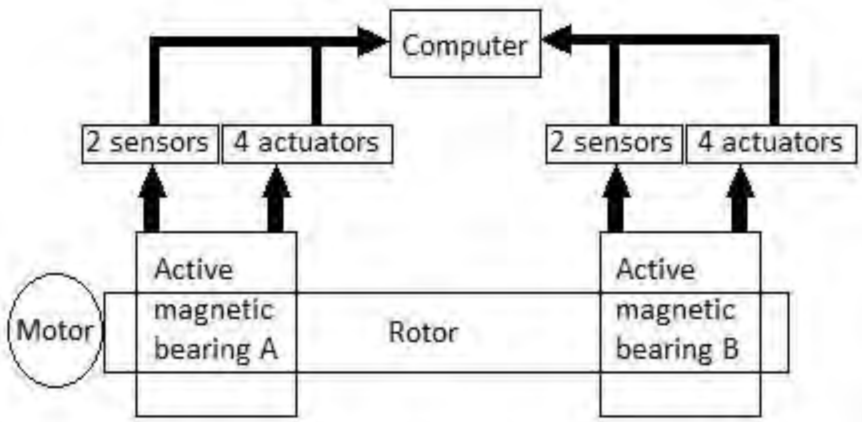

Figure 5.1. System control scheme for the experimental hybrid magnetic bearings.

The position sensors in the active magnetic bearing system are located two for each magnetic bearing, in each one the sensors form an angle of 90 degrees at the imaginary axis point, in Figure 5.2 are shown the signals of the 4 sensors that were located 2 mm away from the rotor , obtaining results of the experimental control system[13] by the PID controller where it is observed the measurement of the sensor does not approach 3 mm, noting that the control system fulfills its role of centering the rotor, and it is concluded that there are overshoots to be reduced using a more precise control that attenuates the signals obtained with the imaginary axis.

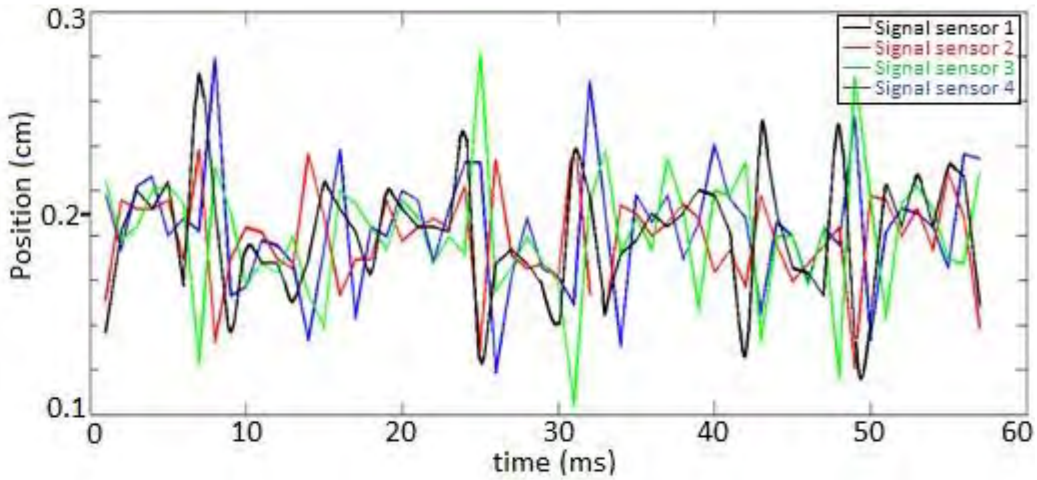

Figure 5.2. Control position for every axis given by classic PI controller [12] With the PI controller, its obtained overshoots, which have to be reduced to obtain the desired position of 2 mm for the system, the overshoots were produced due to the hybrid characteristics of the electromagnetic actuator, for which an optimal predictive control was used to find the correct adaptation coefficients obtaining an optimal position control for the desired position for the system, in the Figure 5.3 shown the 4 signals obtained by the position sensors around the axis, noting notably considering the attenuation with reference to the imaginary axis.

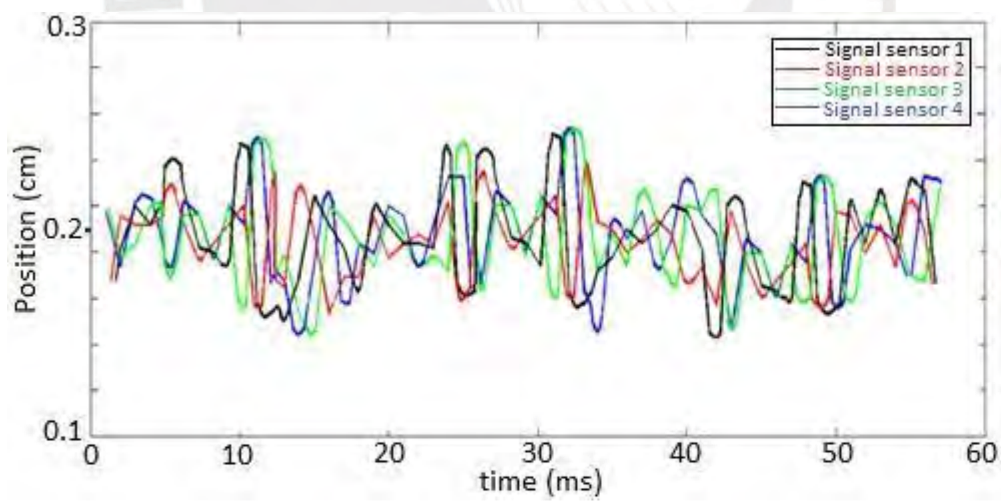

Figure 5.3. Control position for every axis improved by Optimal Controller. [12]

CONCLUTIONS

In this thesis was designed a control algorithm for two hybrid magnetic bearings of 8 electromagnets and 4 position sensors, with a proposed disturbance of a variable load, load that emulates the actual loads of the compressors, transport belts, turbines etc.

For these reason, hybrid magnetic bearings require robust control, which reduces the vibrations of the rotor at the moment of rotation. In the chapter 4 presents the system without control, where is observed a nonlinearity. Therefore, a control system has been realized, that offers better results of stability in the system, in chapter 5, the experimental analysis of the stability hybrid magnetic bearings was used to reduce friction and obtain a better stability, by means of PID cascade controller, which was designed the correct parameters against the mentioned disturbances, obtaining a better position of the rotor with reference to the imaginary axis. It defines that, there are disturbances due to frequency changes in the rotor speed, as well as the disturbances proposed due to the variable load. Due to the changes of speeds, it is observed that the PID controller is not robust, for which an optimal predictive control is used to find the correct coefficients of adaptation, obtaining an optimal position control for the desired position.

REFERENCE

[1] SKF catalogue 2015 “Rodamientos” Svenska Klullagerfabriken AB

[2] Siemens AG 2016. Manual reference “Simiotics Active Magnetic Bearing Technology.

[3] Calderon A. 2019 “Magnetic Bearing Proposal Design for a General Unbalanced Rotor System enhanced because of using sensors/actuators based in nanostructures”, Czech Republic ICPEME 2019 The 3rd International Conference ON POWER, ENERGY AND MECHANICAL ENGINEERING..

[4] Chaowu J. 2016 “Active Magnetic Bearing Stiffness and Damping Identification from Frequency Characteristics of Control System. Hindawi Publishing Corporation Shock and Vibration, Article ID 1067506.

[5] Zhuralev Ju. 2003“Aktivnie Magnitnye Podshipniki” Theory of calculation and application. Book Pp 3-30 Krasnogorskii, Russia, Pskov Polytechnic Institute.

[6] Calderón A. 2016 “Control Strategies for a Prototype of Active Magnetic Bearing System) In Cybernetics, Robotics and Control (CRC), International Conference on, Pp 2226 IEEE.

[7] Aragón D. 2017 “Optimal control for a prototype of an active magnetic bearing system” (Tesis de Maestría). Escuela de Post Grado PUCP, Lima Perú.

[8] Perea F. 2016 “Physical parameters identification for a prototype of Active Magnetic Bearing System” (Tesis de maestría). Escuela de Post Grado PUCP, Lima Perú.

[9] Maslen E., 2009, “Magnetic Bearings” Theory, Design, and Application to Rotating Machinery. Pp. 1-27 Dordrecht Heidelberg London New York, Springer, Schweitzer G.

[10] Se Young Yoon, Zongli Lin, Paul Allaire, 2013 “Control of Surge in Centrifugal Compressors by Active Magnetic Bearings”. Pp 1-4 London Heidelberg New York Dordrecht, Springer.

[11] Zotov I. 2003, “Complex of technical solutions for rotor radial magnetic suspension systems of the horizontal performance turbo generator” Phd thesis, Federal University of Ural, Russia.

[12] Lozano J. 2019 “Control Algorithm Proposal For a Hybrid Magnetic Bearing System With Variable Load”. In Cybernetics, Robotics and Control (CRC), International Conference. USA.

[13] Arredondo I. 2008 “Modelización, Análisis y Control de Sistemas de Cojinetes Magnéticos Activos” Revista Iberoamericana de Automática e informática Industrial ISSN:1679-7912.Vol.5, Nún4,pp17-27.

Appendix A

Initial conditions:

$$Rsin\alpha + FM1sinB = mg \ldots (1)$$

$$Rcos\alpha = FM1cosB \ldots (2)$$

By equilibrium (rotational) R-

reference

$$Lmg = FM1sinB * 2L \ldots(2^*)$$

$$\text{While} \begin{cases} \sum F \rightarrow \frac{\overline{d_r^2}}{d_t^2} \\ \sum F \rightarrow \frac{\overline{d_\theta^2}}{d_t^2} \end{cases} \ldots(3)$$

$$\frac{md_z^2}{dt^2} = R\sin\alpha + FM1\sin B - mg \ldots (4)$$

Where $R \sin \alpha$ y mg- constant

Equation (1) in (4)

$$\frac{md_z^2}{dt^2} = mg - FM_{1_{(0)}} \sin B + FM_1 sinB - mg \ldots (5)$$

Where: $FM_{1(0)}$ initial condition

$$\frac{md_z^2}{dt^2} = (K_Z Z + K_i i) \sin B - (K_z Z_0 + K_i i_0) \sin B \ldots (6)$$

Dynamic equation of the z axis

$$\frac{md_z^2}{dt^2} = K_Z \sin B(Z - Z_0) + K_i sinB(i_i - i_0) \ldots (7)$$

Magnetic force given by this model

$$F_{Mr} = K_r r + K_i I \ldots (8)$$

It is represented

Variable of the current

$$\int_{z_0}^{z} d\,z = z - z_\rho \ldots (9)$$

$$\int_{i_0}^{i} d\,i = i - i_0 \ldots (10)$$

Translation equation,

$$\frac{md_Z^2}{dt^2} = K_Z \sin B(z) + K_i sinB(i\ ) \quad \ldots (11)$$

R- reference

$$\frac{Id_0^2}{dt^2} = -Lmg + 2LFM1sinB \quad \ldots (12)$$

$$\frac{I_Z d_\theta^2}{dt^2} = -L\big(2sinB(K_Z Z_0 + K_i i_0)\big) + 2LsinB(K_Z \mathrm{Z} + K_0 i) \quad \ldots (13)$$

Equation of rotation

$$\frac{I_Z d_\theta^2}{dt^2} = 2LsinBK_z(Z - Z_0) + 2LsinBK_i(i - i_0) \quad \ldots (14)$$

If:

$$\theta = \theta - \theta_0 \ldots (14^*)$$

$$\frac{I_Z d_\theta^2}{dt^2} = 2LsinBK_z(\mathrm{Z}) + 2LsinBK_i(i) \quad \ldots (15)$$

$$l = L\theta \quad \forall\, \theta \to 0 \ \ldots (15^*)$$

$$l \to Z$$

$$\frac{I_Z d_\theta^2}{dt^2} = sinBK_z\theta + 2LsinBK_i i \quad \ldots (16)$$

Joining (11) and equation (16)

Mechanical equation for a system

$$\begin{pmatrix} m & 0 \\ 0 & Iz \end{pmatrix} \begin{pmatrix} \frac{d^2 z}{\mathrm{d}t^2} \\ \frac{d^2\theta}{\mathrm{d}\theta^2} \end{pmatrix} - \begin{pmatrix} K_z sinB & 0 \\ 0 & K_z sinB \end{pmatrix} \begin{pmatrix} \mathrm{Z} \\ \theta \end{pmatrix} = \begin{pmatrix} K_i sinB \\ 2LsinBK_i \end{pmatrix} (\mathrm{i}) \quad \ldots (17)$$

Furthermore i=?

$$v = RI + L\frac{d_I}{dt} \quad \ldots (18)$$

It means (17), (18) Mathematical model AMB

For 2 Electromagnets: (matrix)

$$\begin{pmatrix} m & 0 & 0 & 0 \\ 0 & I_z & 0 & 0 \\ 0 & 0 & m & 0 \\ 0 & 0 & 0 & I_x \end{pmatrix} \begin{pmatrix} \frac{d^2 z}{dt^2} \\ \frac{d^2 \theta_z}{dt^z} \\ \frac{d^2 X}{dt^2} \\ \frac{d^2 \theta_x}{dt^2} \end{pmatrix} -$$

$$\begin{pmatrix} K_z sinB & 0 & 0 & 0 \\ 0 & K_z sinB & 0 & 0 \\ 0 & 0 & K_x sinB & 0 \\ 0 & 0 & 0 & K_x sinB \end{pmatrix} \begin{pmatrix} z \\ \theta_z \\ \mathrm{x} \\ \theta_x \end{pmatrix} =$$

$$\begin{pmatrix} K_i sinB_Z & 0 & 0 & 0 \\ 0 & 2LK_i sinB_Z & 0 & 0 \\ 0 & 0 & K_i sinB_X & 0 \\ 0 & 0 & 0 & 2LK_i sinB_X \end{pmatrix} \begin{pmatrix} i_Z \\ i_Z \\ i_X \\ i_X \end{pmatrix} \ldots (19)$$

$$\Leftrightarrow$$

$$\begin{pmatrix} L_z & 0 \\ 0 & L_x \end{pmatrix} \begin{pmatrix} dI_z \\ dI_x \end{pmatrix} + \begin{pmatrix} R_z & 0 \\ 0 & R_x \end{pmatrix} \begin{pmatrix} I_z \\ I_x \end{pmatrix} = \begin{pmatrix} V_1 \\ V_2 \end{pmatrix} \ldots (20)$$

Appendix B

∀ For all calculation:

$$v_i = I_i R_i + L_i \frac{dI_i}{dt} \Leftrightarrow \mathrm{i} \in [1 \ldots 8]\,;\; i \in z^+ \ldots (21)$$

$$
0\begin{pmatrix} L_1 & 0 & 0 & 0 & 0 & 0 & 0 & 0 \\ 0 & L_2 & 0 & 0 & 0 & 0 & 0 & 0 \\ 0 & 0 & L_3 & 0 & 0 & 0 & 0 & 0 \\ 0 & 0 & 0 & L_4 & 0 & 0 & 0 & 0 \\ 0 & 0 & 0 & 0 & L_5 & 0 & 0 & 0 \\ 0 & 0 & 0 & 0 & 0 & L_6 & 0 & 0 \\ 0 & 0 & 0 & 0 & 0 & 0 & L_7 & 0 \\ 0 & 0 & 0 & 0 & 0 & 0 & 0 & L_8 \end{pmatrix} + \begin{pmatrix} \frac{dL_1}{dt} \\ \frac{dL_1}{dt} \\ \frac{dL_1}{dt} \\ \frac{dL_1}{dt} \\ \frac{dL_1}{dt} \\ \frac{dL_1}{dt} \\ \frac{dL_1}{dt} \\ \frac{dL_1}{dt} \end{pmatrix} +
$$

$$
\begin{pmatrix} R_1 & 0 & 0 & 0 & 0 & 0 & 0 & 0 \\ 0 & R_2 & 0 & 0 & 0 & 0 & 0 & 0 \\ 0 & 0 & R_3 & 0 & 0 & 0 & 0 & 0 \\ 0 & 0 & 0 & R_4 & 0 & 0 & 0 & 0 \\ 0 & 0 & 0 & 0 & R_5 & 0 & 0 & 0 \\ 0 & 0 & 0 & 0 & 0 & R_6 & 0 & 0 \\ 0 & 0 & 0 & 0 & 0 & 0 & R_7 & 0 \\ 0 & 0 & 0 & 0 & 0 & 0 & 0 & R_8 \end{pmatrix} \begin{pmatrix} I1 \\ I2 \\ I3 \\ I4 \\ I5 \\ I6 \\ I7 \\ I8 \end{pmatrix} = \begin{pmatrix} V1 \\ V2 \\ V3 \\ V4 \\ V5 \\ V6 \\ V7 \\ V8 \end{pmatrix} \dots (22)
$$

Solution:

$$v_i = I_i R_i + L_i \frac{dI_i}{dt} \dots (23)$$

Solution by integrals

$$L_i dI_i + I_i R_i \mathrm{dt} = V_i dt \dots (24)$$

$$L_i dI_i = (V_i - I_i R_i) \mathrm{dt} \dots (25)$$

$$L_i \frac{dI_i}{(V_i - I_i R_i)} = dt \text{ ... } (26)$$

Where:

$$V_i - I_i R_i = Z_i \dots (27)$$ Deriving

with respect to the current:

$$\frac{dV_i}{dI_i} - \frac{d}{dI_i}(R_i I_i) = \frac{d}{dI_i}(Z_i) \dots (28)$$

$$\Leftrightarrow \quad \frac{dV_i}{dI_i} = 0;$$

V_i=V=cte

$$0 - R_i \frac{I_i}{dI_i} = \frac{dZ_i}{dI_i} \text{ … (29)}$$

$$dZ_i = -R_i dI_i \text{ … (30)}$$

(27) and (30) in (26)

$$L_i \frac{1}{Z_i}\left(-\frac{1}{R_i} dZ_i\right) = dt \text{ … (31)}$$

$$\frac{-L_i}{R_i}\frac{dz_i}{z_i} = d_t \text{ … (32)}$$

$$\frac{dz_i}{z_i} = -\frac{R_i}{L_i} dt \text{ … (33)}$$

$$Ln\, Z \int_{z_0}^{z_i} = -\frac{R_i}{L_i}(t - t_{0)} \text{ … (34)}$$

$$L_n|z_i| - Ln|z_0| = -\frac{R_i}{L_i}(t - t_{0)}) \text{ … (34)}$$

$$L_n\left(\frac{Z_i}{Z_0}\right) = -\frac{R_i}{L_i}(t - t_{0)}) \text{ … (35)}$$

$$\frac{Z_i}{Z_0} = e^{-\frac{R_i}{L_i}(t-t_0)} \text{ … (36)}$$

$$\frac{V_i - R_i I_i}{V_i} = e^{-\frac{R_i}{L_i}(t-t_0)} \text{ … (37)}$$

$$V_i = R_i I_i + V_i e^{-\frac{R_i}{L_i}(t-t_0)} \text{ … (38)}$$

$$R_i I_i = V_i - V_i e^{-\frac{R_i}{L_i}(t-t_0)} \text{ … (39)}$$

$$I_i = \frac{V_i}{R_i}(1 - e^{-\frac{R_i}{L_i}(t-t_0)}) \text{ …(40)}$$

It´s know following model:

$$m \frac{d^2x(t)}{dt^2} + \gamma \frac{dx(t)}{dt^2} + kx_t = 0 \text{ … (41)}$$

$$1 \frac{d^2x}{dt^2} + \frac{\gamma}{m}\frac{dx(t)}{dt} + \frac{k}{m} x_{(t)} = 0 \text{ …(42)}$$

Where values replace them:

1=a

$$\frac{\gamma}{m} = b \text{ … (43)}$$

$$\frac{k}{m} = c \text{ … (44)}$$

Model over damping $\Leftrightarrow b^2 - 4ac > 0 \{ \; y(t) = e^{-\frac{b}{2}t}(A\, e^{\Omega t} + Be^{-\Omega t})$… (45)

$$\Leftrightarrow \Omega = \sqrt{\left(\frac{b}{2}\right)^2 - c} \ldots (46)$$

Damping $\Leftrightarrow b^2 - 4ac = 0 \{ \ y(t) = e^{-\frac{b}{2}t}(A \ + Bt\ ) \ldots (47)$

Under damping $\Leftrightarrow b^2 - 4ac < 0 \{ \ y(t) = e^{-\frac{b}{2}t}(A\cos\Omega + Bsin\,\Omega t\ ) \ldots (48)$

$$\Leftrightarrow \Omega = \sqrt{i - \left(\frac{b}{2}\right)^2} \ldots (49)$$ Solving

the know model:

$$m\frac{d^2x(t)}{dt^2} + \gamma\frac{dx(t)}{dt^2} + kx_t = 0 \ldots (50)$$

$$x(t) = c_1e^{at} + C_2e^{bt} \ldots (51)$$

$$\frac{dx(t)}{dt} = c_1ae^{at} + C_2be^{bt} \ldots (52)$$

$$\frac{d^2x(t)}{dt^2} = c_1a^2e^{at} + C_2b^2e^{bt} \ldots (53)$$

(52) and (53) in (41)

$$m(c_1a_2e_{at} + C_2b_2e_{bt}) + \gamma(c_1ae_{at} + C_2be_{bt}) + k(c_1e_{at} + C_2e_{bt}) =$$

Isomorphism to solve

$$c_1(ma^2 + \gamma a + k)e^{at} + c_2(mb^2 + \gamma b + k)e^{bt} = 0$$

Performing a Laplace inverse transform l^{-1}

$$c_1(ma^2 + \gamma a + k)\frac{1}{s-a} + c_2(mb^2 + \gamma b + k)\frac{1}{s-b} = 0 \ldots (54)$$

$$c_1(ma^2 + \gamma a + k)(s - b) + c_2(mb^2 + \gamma b + k)(s - a) = 0 \ldots (55)$$

Comparisons to find the parameters

... s +... =... s+ ... Solving

the coefficients to demonstrate the three cases:

$$ma^2 + \gamma a + k \ldots (56)$$

$$\Delta = \frac{-\gamma \pm \sqrt{\gamma^2 4(m)(k)}}{2m} \ldots (57)$$

System identification

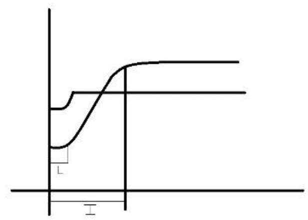

$$\frac{y_{(s)}}{U_{(s)}} = \frac{\text{kp}}{Is+1} e^{-Ls} \Leftrightarrow L < I \quad \ldots (58)$$

$$Iy_{(s)} + y_{(s)} = \text{kp}U_{(s)} \ldots (59)$$

$\frac{Idy(t)}{dt} + y_{(t)} = \text{kp}U_{(t)}$ – by theory

$\frac{ady(t)}{dt} + by_{(t)} = cU_{(t)}$ – by experience

Modulated Functions

$$a_1 d^n \frac{p(t)}{dt^n} + a_2 d^{n-1} \frac{p(t)}{dt^{n-1}} + a_3 d^{n-2} \frac{p(t)}{dt^{n-3}} + \cdots am = F(t) \quad \ldots (60)$$

$$Y(t) = ?$$

American model:

Responses in time by excitation (frequencies or spectrum, depends on the type of calibration)

Analysis: Rotation tendency with degree of freedom.

$$\begin{pmatrix} m & 0 \\ 0 & I \end{pmatrix} \begin{pmatrix} \frac{d^z(t)}{dt^2} \\ \frac{d^z \theta_2(t)}{dt^2} \end{pmatrix} - \begin{pmatrix} k_z sinB & 0 \\ 0 & k_z sinB \end{pmatrix} \begin{pmatrix} z \\ \theta_z \end{pmatrix} = \begin{pmatrix} k_i sinB & 0 \\ 0 & 2l sinBki \end{pmatrix} \begin{pmatrix} i_z \\ i_z \end{pmatrix} \quad \ldots (61)$$

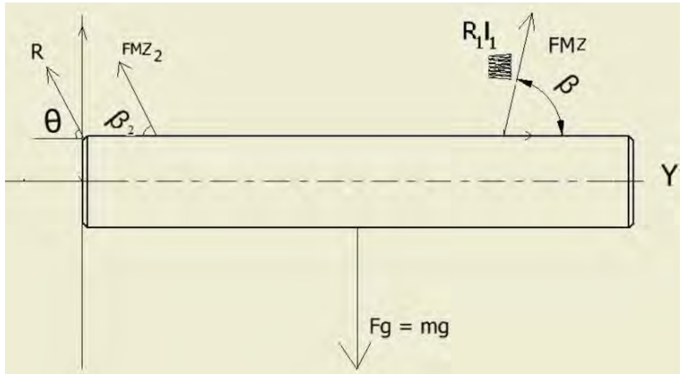

Figure 2.5: Sample of the shaft with a force that is produced by 1 active magnetic bearing.

Working for:

$$md^2\frac{z(t)}{dt^2} - k_z sinBZ_t = k_i \sin Bi_b \quad \ldots (62)$$

$$md^2\frac{z(t)}{dt^2} - k_z sinBZ_t = k_i \sin B[\frac{v_0}{R}\left(1 - e^{\frac{-R_1}{L_1}(t-t_0)}\right)] \quad \ldots (63)$$

Therefore, to solve this differential equation to archive geometrical parameters for one magnet effect.

$$Z(t) = z_h^{(t)} + z_P^{(t)} \quad \ldots (64)$$

$$z_h^{(t)} = ?$$

$$md^2\frac{z(t)}{dt^2} - k_z sinBZ_t = 0 \quad \ldots (65)$$

$$1\frac{d^2z(t)}{dt^2} + \frac{0}{m}\frac{dz(t)}{dt} - \frac{k_z}{m}sinBZ_{(t)} = 0 \quad \ldots (66)$$

Where:

a= 1 b

$$= \frac{0}{m}$$

$$c = -\frac{k_z}{m}sinB \quad \ldots (67)$$

$$F = k_z I + k_z Z \ldots (68)$$

$$b^2 - 4ac = 0^2 - 4(1)\left(-\frac{k_z}{m}sinB\right) = \frac{4k_z}{m}sinB \quad \ldots (69)$$

$\Leftrightarrow k_z > 0$ (Over damping)

The sign must be positive, if it´s negative it implies that system is not stable.

$$\Leftrightarrow \; \Omega = \sqrt{\left(\frac{b}{2}\right)^2 - c} \; \ldots (70)$$

A, B, there are obtained through 2 conditions

$$\Omega = \sqrt{\frac{1}{4}(0) - 4(1)(-\frac{kz}{m}sinB)} \ldots (71)$$

$$\Omega = 2\sqrt{\frac{kz}{m}sinB} \ldots (72)$$

$$z(t) = Ae^{2\sqrt{\frac{k_Z.\sin B}{m}}.t} + Be^{-2\sqrt{\frac{k_Z.\sin B}{m}}.t} \ldots (73)$$

$$Z(t_0 = 0) = A + B = Z_0 \ldots (74)$$

$$Z_P(t) = ?$$

$$Z_P = K_i limp(1 - e^{\frac{-R_1}{L_1}(t)}) \ldots (75)$$

$$Z_P(t) = D + e^{-\text{ft}} \ldots (76)$$

$$\frac{dZ_P(t)}{dt} = -Fe^{-\text{ft}} \ldots (77)$$

$$\frac{dz^2p(t)}{dt^2} = +F^2e^{-\text{ft}} \ldots (78)$$

$$m\left(F^2e^{-\text{ft}}\right) - k_z.\sin B\left(D + e^{-\text{ft}}\right) = k_i.\sin B\frac{V_0}{R_1} - k_i.\sin B\frac{V_0}{R_1}e^{\frac{-R_1}{L_1}}t$$

$$-k_z.\sin B\, De^{-\text{ft}}(mF^2 - KzsinB) = k_i.\sin B\frac{V_0}{R_1} - k_i.\sin B\frac{V_0}{R_1}e^{\frac{-R_1}{L_1}}t$$

$$D = -k_i.\frac{V_0}{R_1 k_Z} \ldots (79)$$

$$\text{F} = \frac{R_i}{4} \ldots (80)$$

$$mF^2 - KzsinB = -k_i.\sin B\frac{V_0}{R_1} \ldots (81)$$

State of the rotor, mass m:

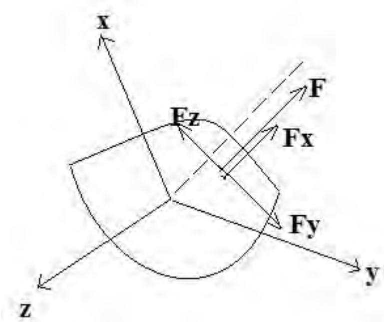

$$Md^2\frac{r(t)}{dt^2} = \frac{dF_{(t)}}{dt} \dots (82)$$

$$U_{(t)} = \frac{dF_{(t)}}{dt}$$

$$MA = U_{(t)}$$

If:

$$F = F_1 + F_2$$

$$\rightarrow r = f(x, y, z)$$

$$r = f(x_1x_2, y_1y_2, z_1z_2) \dots (83)$$

$$F = F_1 + F_2 + F_3 + \cdots + F_n \dots (84)$$

$$r \rightarrow f(x_1x_2, x_3, \dots x_n, y_1, y_2, y_3, \dots, y_n, z_1, z_2, z_3, \dots, z_n)$$

$$\vec{r} = \vec{f}(\bar{x}_N, \bar{y}_N, \bar{z}_N)$$

$$\gamma = \frac{dF_{(t)}}{dt} \neq 0 \dots (85)$$ In

our case:

$$a\frac{d^2z(t)}{dt^2} + bz = D + fg(t) \dots (86)$$

$$a\frac{d^2z(t)}{dt^2}\gamma\frac{dz(t)}{dt} + bz = D + fg(t) \dots (87)$$

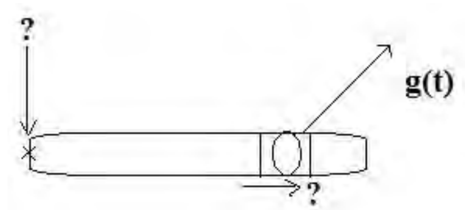

v? - reference point

$$z(t) = [x(t), y(t), \Theta(t), \phi(t)]^T$$

$$\begin{pmatrix} a & 0 & 0 & 0 \\ 0 & a & 0 & 0 \\ 0 & 0 & a & 0 \\ 0 & 0 & 0 & a \end{pmatrix} \frac{d}{dt} \begin{pmatrix} x(t) \\ y(t) \\ \Theta(t) \\ \phi(t) \end{pmatrix} + \begin{pmatrix} \gamma & 0 & 0 & 0 \\ 0 & \gamma & 0 & 0 \\ 0 & 0 & \gamma & 0 \\ 0 & 0 & 0 & \gamma \end{pmatrix} \begin{pmatrix} x(t) \\ y(t) \\ \Theta(t) \\ \phi(t) \end{pmatrix} + \begin{pmatrix} x(t) \\ y(t) \\ \Theta(t) \\ \phi(t) \end{pmatrix} =$$

$$\begin{pmatrix} D_{1,} \\ D_{2,} \\ D_{3,} \\ D_{4,} \end{pmatrix} \begin{pmatrix} b & 0 & 0 & 0 \\ 0 & b & 0 & 0 \\ 0 & 0 & b & 0 \\ 0 & 0 & 0 & b \end{pmatrix} \begin{pmatrix} g1(t) \\ g2(t) \\ g3(t) \\ g4(t) \end{pmatrix} \ldots (88)$$

So in this case while:

$$z(t) = [x_1 x_{2,} x_3, \ldots x_{n,} y_1, y_{2,} y_3, \ldots, y_{n,} \Theta_1, \Theta_2, \Theta_3, \ldots, \Theta_n, \phi_1, \phi_2, \phi_3, \ldots, \phi_n,]^T \ldots (89)$$

$$A\ddot{z}_{(t)} + A\dot{z}_{(t)} + Bz_t = D^* + FG_{(t)} \ldots \; (90)$$ General

equation:

$$md^2 \frac{z(t)}{dt^2} - k_z sinBZ_{(t)} = k_i sinBi_{(t)} \ldots \; (91)$$

$md^2 \frac{z(t)}{dt^2}$: Is the mass multiplying the derivative of the position

$$\Leftrightarrow i(t) = \frac{V_0}{R} - \frac{V_0}{R} e^{\frac{-R}{L}(t-t_0)} \ldots \; (92)$$ To

solve this differential equation for a one point:

$$z_{(t)} = \left(Ae^{\sqrt{k_z B_t}} + Be^{-\sqrt{k_z B_t}}\right) + (D + Ee^{-gt}) \ldots (93)$$

$$D = \frac{V_0}{k_z} \frac{k_i}{R} \ldots (94)$$

$$E = \frac{k_i B V_0}{R(m(\frac{R}{L})^2 - k_z B} \ldots (95)$$

B=90° or 0°

$$F_M = k_Z Z + k_i i \ldots (96) \; mg$$

$$= 2Fm \ldots (97)$$

2.3 Analysis of electrical components:

Initial conditions:

$$i_0 = mg \ldots (98)$$

$$\Theta\ be\ flexible$$

$$\Theta \rightarrow 45°$$

$$[k_i] \sim 1$$

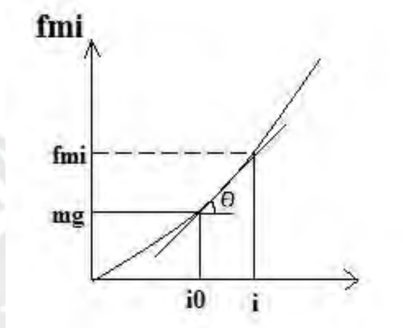

Where: mg= 1kg

i0=10A

$i = \in [10 \ldots 30]A$

Diameter of the current wire: 1mm

10A→m(10)

$$m \sim 1kg$$

For Kz

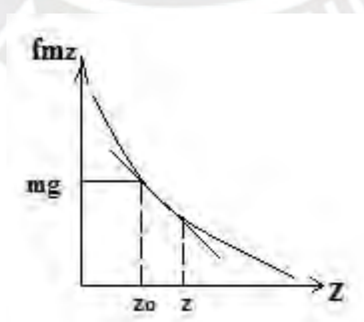

Trend lineal:

$$F_{Mz} \rightarrow k_Z(Z - Z_0) \ \dots$$ (99) Magnetic

force:

$$F_M = f_{mi} + f_{mz} \dots$$ (100)

$$F_M = k_i(i - i_0) + k_z(z - z_0) \ \dots$$ (101)

$$0.5\ mg = (i - 10) + (z - z_0) \ \dots$$ (102)

$z = 0.001m\dots$ requirement

$z_0 = 0.0003m..$ proposal

$$5 = i - 10 + 0{,}007\dots$$ (103)

$$i \sim 14.993$$

Appendix C

This is a conductive wire for the electromagnetic coil.

CONDUCTORES DESNUDOS

Descripción
Conductores de cobre electrolítico de 99,99% de pureza mínima, recocido, semiduro y duro. Sólidos (alambres) y cableados concéntricamente.

Usos
Alambres duros: Circuitos aéreos de comunicación telegráfica y otros usos.
Alambres recocidos: En sistemas de puesta a tierra.
Cables duros: En líneas aéreas de transmisión y redes de distribución aérea.
Cables recocidos: En sistemas de puesta a tierra, protección de equipos y aplicaciones de uso general.

Norma de Fabricación

Alambre	: NTP 370.251.
Cables de cobre duro	: NTP 370.251.
Cables de cobre recocido	: NTP 370.251.
Cables de cobre semiduro	: NTP 370.251.
	: ASTMB8
	: ASTMB2

Calibre
Alambres: 0.5mm² - 16 mm²
Cables: 1.5mm² - 500 mm²

INDECO
empresa Nexans

JORVEX

01 WP (CPI)

DESCRIPCIÓN	NORMA DE FABRICACIÓN
Conductor de cobre electrolítico duro de 99.9% de pureza, cubierta protectora de polietileno termoplástico negro resistente a la intemperie y envejecimiento.	ITINTEC 370.045 (Calibre mm2) ANSI C8 - 35 (Calibres AWG - MCM)
	TENSIÓN DE SERVICIO
	Depende de los aisladores utilizados en su instalación.
USOS	**TEMP. DE OPERACIÓN**
Redes de distribución primaria y secundaria. Tendidos a la intemperie en plantas industriales, minas, etc. Tensiones mayores o iguales a 600 V., requiere aisladores.	75° C.
	CALIBRES
	6 - 185 mm² 14 AWG - 300 mcm

Sensor Sharp

SHARP GP2Y0A21YK0F

GP2Y0A21YK0F

Distance Measuring Sensor Unit
Measuring distance: 10 to 80 cm
Analog output type

■Description

GP2Y0A21YK0F is a distance measuring sensor unit, composed of an integrated combination of PSD (position sensitive detector) , IRED (infrared emitting diode) and signal processing circuit.
The variety of the reflectivity of the object, the environmental temperature and the operating duration are not influenced easily to the distance detection because of adopting the triangulation method.
This device outputs the voltage corresponding to the detection distance. So this sensor can also be used as a proximity sensor.

■Features

1. Distance measuring range : 10 to 80 cm
2. Analog output type
3. Package size : 29.5×13×13.5 mm
4. Consumption current : Typ. 30 mA
5. Supply voltage : 4.5 to 5.5 V

■Agency approvals/Compliance

1. Compliant with RoHS directive (2002/95/EC)

■Applications

1. Touch-less switch
   (Sanitary equipment, Control of illumination, etc.)
2. Robot cleaner
3. Sensor for energy saving
   (ATM, Copier, Vending machine)
4. Amusement equipment
   (Robot, Arcade game machine)

Is a requirement of the prototype.

NO Readme Files

Series NO PM12-04P
Name:Inductive Proximity Sensor

Descripting
M12 Sensing Direction-4.0mm

PRODUCT DESCRLPTLON

Model	Output Status	Output Method	Operating Voltage	Sensing Distance	Response Frequency	Mounting Method
PM12-04N	NO	NPN	10~30VCD	4.0mm	2.5KHZ	Non-Flushed
PM12-04NB	NC	NPN				
PM12-04P	NO	PNP				
PM12-04PB	NC	PNP				

http://www.photosensor.com.tw

Sensor capacitivo
BC10-P30SR-VP4X2/3GD

TURCK
Industrial Automation

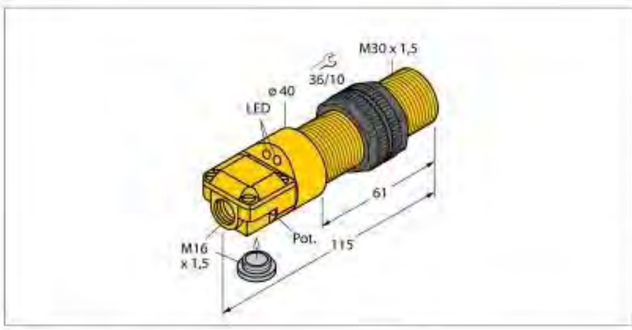

- **ATEX categoría II 3 G, zona Ex 2**
- **ATEX categoría II 3 D, Ex zona 22**
- **Tubo roscado, M30 x 1,5**
- **Plástico, ABS**
- **Sensibilidad ajustable por potencióme-tro**
- **4 hilos CC, 10…65 VCC**
- **Contacto de conmutación, salida PNP**
- **Compartimento de bornas**

Designación de tipo	BC10-P30SR-VP4X2/3GD
N° de identificación	2505006
Distancia de detección (a ras)	10 mm
Distancia de conmutación de referencia (no a ras)Sn	15 mm
Distancia de conmutación asegurada	≤ (0,72 x Sn) mm
Histéresis	2…20 %
Variación de temperatura	Tipo: 20 %
Precisión de repetición	≤ 2 % v. f.
Temperatura ambiente	-25…+70 °C

Diagrama de cableado

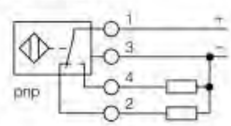

Principio de funcionamiento

Los sensores capacitivos están diseñados para la detección de objetos metálicos (eléctricamente conductores) y no metálicos (no conductores) sin contacto ni desgaste.

Tensión de servicio	10…65 VCC
Ondulación residual	≤ 10 % U_{ss}
Corriente DC nominal	≤ 200 mA
Corriente sin carga I_0	≤ 15 mA
Corriente residual	≤ 0.1 mA
Frecuencia de conmutación	0.1 kHz
Tensión de control de aislamiento	≤ 0.5 kV
Salida eléctrica	4 hilos, Contacto antivalente, PNP
Protección cortocircuito	sí/ cíclica
Fallo de la tensión en I_e	≤ 1.8 V
Protección ante corto-circuito/polaridad inversa	sí/ completa
Aprobación conforme	declaración de conformidad ATEX 3146M
Identificación del aparato	Ⓔ II 3 G EEx nA II T4 X / II3 D IP67 T 90 ℃
Aviso	Utilizar atornilladuras con autorización ATEX.
Diseño	Tubo roscado, M30 × 1.5
Material de la cubierta	Plástico, ABS
Material de la cara activa	plástico, ABS, amarillo
Presión admisible en capuchón frontal	≤ 3 bar
par de apriete máx. de la tuerca de la carcasa	5 Nm
Conexión eléctrica	Caja de bornes
Resistencia a la vibración	55 Hz (1 mm)
Resistencia al choque	30 g (11 ms)
Grado de protección	IP67
MTTF	1080 Años según SN 29500 (ed. 99) 40 °C
Indicación estado de conmutación	LED

Appendix D

ANALYSIS OF PARAMETERS CALCULATED MATHEMATICALLY WITH PARAMETERS OBTAINED EXPERIMENTALLY:

The DAQ, of national instruments module will be used to obtain the acquisition data with sensor SHARP.

The electronic components used for this test are:

Power supply 12v

Motor and axis of prototype of active magnetic bearing controlling an axis by author ARAGON, motor high and low speed.

Potentiometer 1M regulated to 200 ohms

Led

Relay Protoboard

Sensor Sharp.

Performing the test and obtaining the following data by the data acquisition DAQ of national instruments.

The test one is done with a voltage of 2.5 and with a current of 1.68 amps that comes to be the low speed of the motor and the test 2 is done with a voltage of 2.5 and with a current of 1.70 amps that comes to be the speed high engine.

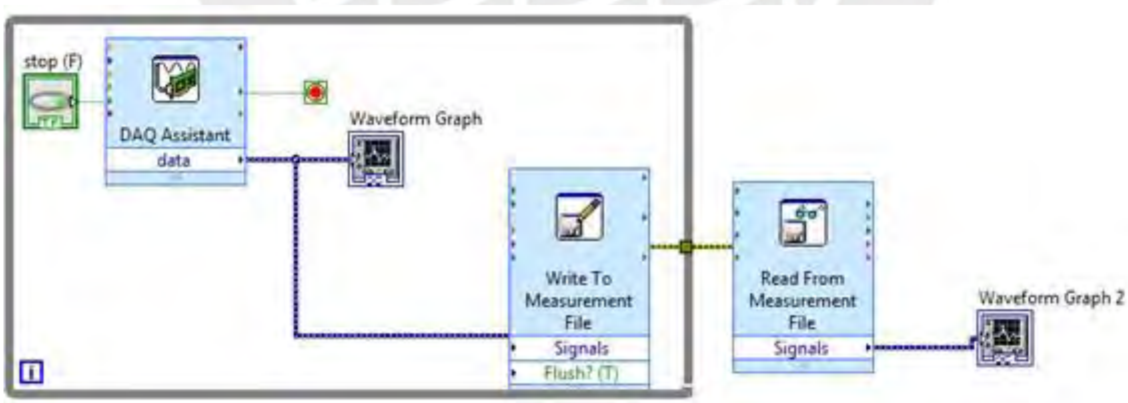

Figure 5.1 Program for data sampling using national instrument software.

Data obtained from the sample of parameters without electromagnetic coils control:

1 Engine test with low speed:

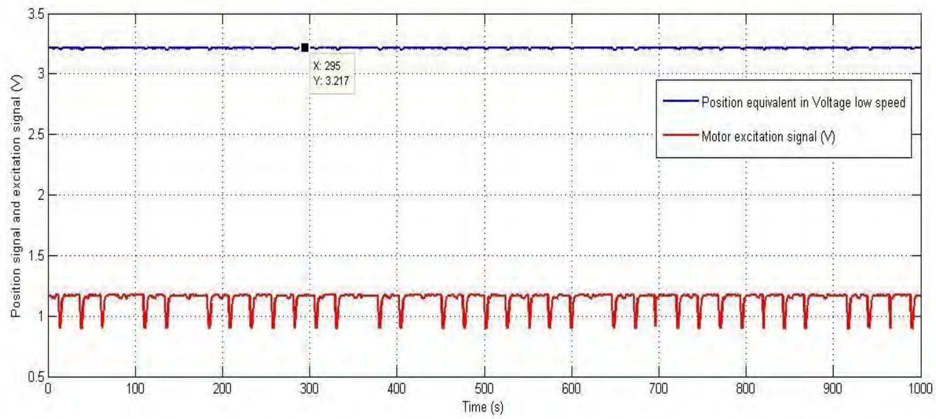

Figure 5.2 Sensor response SHARP with a motor at low speed

2 Engine test with high speed:

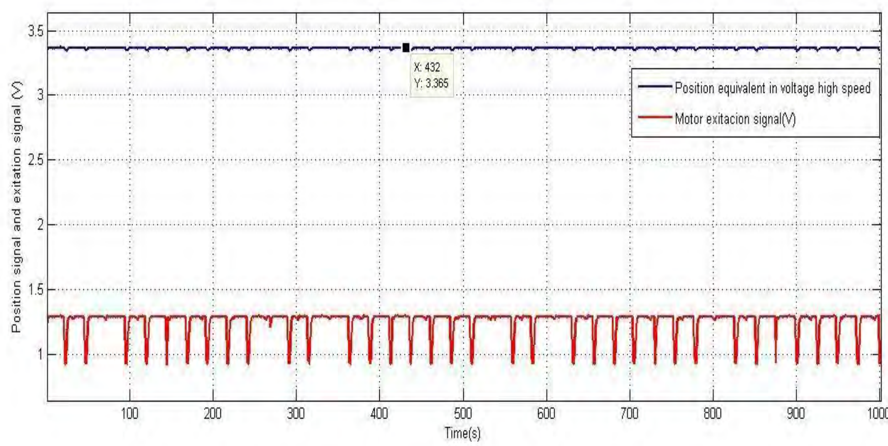

Figure 5.3 Sensor response SHARP with a motor at high speed.

In both cases of the test shown and the answers obtained, there is noise in the signal that must be filtered to obtain the data with precision, for which a control system is needed. For which is going to take the reference of sensing for the sampling of the signal of the following way: We Will use two SHARP sensors located around the rotor to be sensed, the angle of position between them Will be 90 degrees, in the same way we Will use two electromagnetic coils located perpendicular to the sensors that when activated, will produce forces that Will make the signal obtained at the beginning change since there are forces that modify the initial response obtained.